



## Machine Learning Assisted Provisioning of Time-Varying Traffic in Translucent Optical Networks

Downloaded from: <https://research.chalmers.se>, 2024-09-27 07:32 UTC

Citation for the original published paper (version of record):

Włodarczyk, A., Knapinska, A., Lechowicz, P. et al (2024). Machine Learning Assisted Provisioning of Time-Varying Traffic in Translucent Optical Networks. IEEE Access, 12: 110193-110212.  
<http://dx.doi.org/10.1109/ACCESS.2024.3441522>

N.B. When citing this work, cite the original published paper.

© 2024 IEEE. Personal use of this material is permitted. Permission from IEEE must be obtained for all other uses, in any current or future media, including reprinting/republishing this material for advertising or promotional purposes, or reuse of any copyrighted component of this work in other works.

Received 18 June 2024, accepted 3 August 2024, date of publication 9 August 2024, date of current version 19 August 2024.

Digital Object Identifier 10.1109/ACCESS.2024.3441522

## RESEARCH ARTICLE

# Machine Learning Assisted Provisioning of Time-Varying Traffic in Translucent Optical Networks

ADAM WŁODARCZYK<sup>1</sup>, ALEKSANDRA KNAPIŃSKA<sup>1</sup>, (Member, IEEE),  
PIOTR LECHOWICZ<sup>1,2</sup>, (Member, IEEE), AND  
KRZYSZTOF WALKOWIAK<sup>1</sup>, (Senior Member, IEEE)

<sup>1</sup>Department of Systems and Computer Networks, Wrocław University of Science and Technology, 50-372 Wrocław, Poland

<sup>2</sup>Department of Electrical Engineering, Chalmers University of Technology, 412 96 Gothenburg, Sweden

Corresponding author: Adam Włodarczyk (Adam.Wlodarczyk@pwr.edu.pl)

This work was supported by the National Science Center (NCN), Poland, under Grant 2019/35/B/ST7/04272.

**ABSTRACT** The overall network volume in backbone optical networks is constantly growing, composed of many smaller network services with increasing trends and various seasonality. Due to the recent advances in machine learning algorithms, short- and long-term traffic fluctuations can be forecasted. Consequently, the backbone optical network can be adapted to traffic changes aiming to improve its performance. However, an important challenge lies in developing effective optimization methods capable of adapting to traffic changes to leverage the knowledge about the traffic. To this end, this paper addresses the time-varying traffic in spectrally-spatially flexible optical networks (SS-FONs), which are a promising technology to mitigate backbone network requirements of vast traffic volume transmission. The main contribution of this paper is twofold. Firstly, we introduce a new traffic prediction method using multioutput regression and temporal features to forecast traffic between all node pairs and integrate this prediction method into an optimization framework developed for dynamic resource allocation in translucent SS-FONs with time-varying traffic. Secondly, we evaluate potential network performance improvements from periodic lightpath reallocation through extensive numerical experiments. According to the results of experiments run on two representative optical network topologies, the proposed approach with periodic resource allocation allows achieving up to 7.8 percentage points reduction of bandwidth blocking compared to the reference scenario without reallocation. Consequently, the network requires up to 23.4% fewer transceivers to deliver the same traffic in considered scenarios and thus the power consumption savings are provided.

**INDEX TERMS** Machine learning, routing and spectrum allocation, translucent optical networks, time-varying traffic, traffic prediction.

## I. INTRODUCTION

According to many statistics and reports, the Internet traffic carried in backbone optical networks connecting the world is time-varying across the day. For instance, *The Mobile Internet Phenomena Report* published by Sandvine [1] presents hourly trends of various mobile services and applications, including video streaming, social media, YouTube, TikTok,

The associate editor coordinating the review of this manuscript and approving it for publication was Rentao Gu<sup>1</sup>.

Snapchat, and Zoom. Moreover, the *Nokia Deepfield Network Intelligence Report* [2] shows many examples of traffic patterns from various service providers (aggregated traffic and various categories of traffic) around the world, indicating the 24-hour seasonality. Finally, the Seattle Internet Exchange (SIX) [3] interconnecting hundreds of networks and data centers and carrying more than 2 Tbps of peak bitrate provides traffic reports since 1997 showing how the traffic changes over the day. All these mentioned examples clearly show that the optical network traffic is time-varying and

changes over the day, which is a function of human activity.

Meanwhile, numerous parameters of the networks are profoundly monitored, thus generating enormous amounts of valuable data. With the recent development of artificial intelligence (AI), specifically machine learning (ML) techniques, those measurements can be used to enhance various aspects of network operation [4], [5]. In particular, quality of transmission (QoT) estimation [6], [7], fragmentation and defragmentation problems [8], [9], or link dimensioning and bandwidth blocking estimation [10], [11] are just a few examples of the currently explored research directions in the networking community. However, one of the essential issues is short- and long-term traffic prediction. Prior knowledge about the future traffic can improve routing decisions, thus reducing blocking probability and resource utilization [12], [13], [14] or enabling accurate planning of long-term network upgrades [15], [16].

Due to the fact that the overall Internet traffic increases constantly, which can lead to incremental exhaustion of available capacity and to facilitate the network operation, several solutions for optical networks have been proposed in recent years. Space division multiplexing (SDM) is an optical network technology that exceeds the capacity provided by spectrally-flexible (elastic) optical networks (EONs) by supporting parallel transmission of co-propagating spatial modes in properly designed optical fibers. Spectrally-spatially flexible optical network (SS-FON) is a combination of SDM with EON technologies. SS-FONs offer a number of advantages, including a huge growth in transmission capacity, translucent transmission of the optical signal with regeneration in certain nodes of the route, flexibility in resource management, and prospects of cost savings [17].

Moreover, in recent years, energy efficiency has become a significant challenge for the entire ICT sector, including optical networks. Therefore, research on optimizing optical networks should address, among other requirements, how to achieve power savings while maintaining a bandwidth blocking ratio comparable to that of earlier approaches [18].

It should be noted that most of the previous research on the optimization of optical networks has not addressed the fact that the network traffic is time-varying and changes throughout the day. Therefore, the main contribution and key novelty of this paper is that we propose an effective optimization approach for translucent SS-FONs that takes advantage of the specific characteristics of time-varying traffic. This is achieved in two ways. First, the proposed optimization approach using periodic reallocation of lightpaths allows the allocated SS-FON resources to adjust to the changing traffic over time in order to improve network performance. Second, based on the patterns included in the time-varying traffic (e.g., seasonality), we enhance the proposed optimization framework with traffic prediction based on ML methods.

The main contributions of the paper are as follows:

- Development of a new traffic prediction method for traffic between all pairs of nodes based on multioutput

regression and temporal features. This method includes two approaches for forecasting various reallocation periods and is incorporated into an optimization framework that allows dynamic allocation of resources in a translucent optical network with time-varying traffic.

- Assessing the potential improvements in network performance (higher network capacity and smaller power consumption of transceivers) due to the periodic reallocation of lightpaths through extensive numerical experiments.

The rest of the paper is organized as follows. Section II presents related works. Section III introduces the considered network model and traffic model. Section IV describes the proposed heuristic algorithm. Section V focuses on traffic prediction. Section VI presents the results of numerical experiments and discusses the results obtained. Finally, the last Section VII concludes this work.

## II. RELATED WORKS

In this Section, we discuss the literature related to various aspects of our work, i.e., dynamic optimization methods of translucent SS-FONs, consideration of the time-varying nature of network traffic, and traffic prediction with traffic-prediction-aided network optimization methods.

### A. DYNAMIC OPTIMIZATION OF TRANSLUCENT SS-FONS

One of the fundamental operations in optical networks is the provision of lightpaths for traffic requests. Despite the routing decision, various other constraints may be imposed depending on the applied network architecture. To reduce network cost, previously opaque optical networks are replaced with translucent (with O-E-O regeneration in some nodes) or transparent (all-optical) ones [19]. If requests are known in advance, the routing algorithms are called as *static* or *offline* [20], while when the network serves dynamically incoming traffic, or traffic that changes over time without prior knowledge of those changes, the problem is called as *dynamic* or *online* [21]. In the static case, lightpaths are served on a semi-permanent basis, allowing the use of advanced, time-consuming methods, such as integer linear programming (ILP), for finding exact solutions [22], or ILP relaxation [20] and metaheuristic algorithms [22] (often without any optimality guarantee). On the contrary, for dynamic traffic, the decision needs to be taken almost immediately; thus, various heuristic approaches are often used [21], [23].

In SS-FONs, the fundamental connection provisioning problem is called routing, spectrum, and space assignment (RSSA), where for each traffic request, a routing path and a suitable optical corridor are assigned occupying one or more spectrum slots and one or more spatial resources [17], [24], [25], [26], [27]. If the transmission is realized over specific spatially-enabled fibers [28], such as multi-core fibers or multi-mode fibers, then the problem is called routing, spectrum, and core assignment (RSCA) and routing, spectrum, and mode assignment (RSMA) [23], respectively.

In addition, modulation format selection can be incorporated into the problem of creating routing, modulation, spectrum, and core allocation (RMSCA) [29]. In the literature, one of the approaches is to divide this problem into two smaller subproblems, namely, the routing problem and the spectrum (spatial) assignment problem [17], [30], [31], [32]. In the routing subproblem, the available routes for the request can either be precomputed (static) or calculated during the execution of the algorithm (dynamic) based on the network state (e.g., based on the congestion in network links). Commonly used static routing algorithms are fixed routing (e.g., shortest path), fixed alternate routing (e.g., k-shortest paths), and least congested routing (with fixed precomputed shortest paths on which congestion is evaluated at run-time), while the dynamic one is adaptive shortest path routing where the path is computed based on the current network state parameters treated as graph weights. In the second subproblem, namely, the spectrum assignment problem, the decision is taken which spectral slots should be assigned to the selected routing path to form the lightpath. The most common approaches are first fit, random fit, last fit, first-last fit, least used, most used, and exact fit [30], [32].

### B. CONSIDERATION OF TIME-VARYING TRAFFIC

The traffic offered to the network, e.g., to the IP layer, is composed of small requests for which the bit-rate fluctuates over time [31]. These traffic volume fluctuations are often correlated with time, and patterns can be observed based on time horizons, e.g., day, week, month, year [2], [33], [34]. However, the majority of works do not consider time-varying traffic and assume that it is constant over time. Nevertheless, such changes can be either processed in IP layer by, e.g., grooming requests [35], [36], establishing sufficiently large lightpaths in the optical layer [37], or by dynamically changing spectrum in optical layer and sharing some spectral resources [32]. Based on the flexibility in changing spectral resources, one can distinguish fixed spectrum allocation where request (requests) can utilize the whole or fraction of the established optical corridor, and the spectrum assigned to the lightpath does not change when the request's bit-rate changes. In semi-elastic spectrum allocation, the width of the spectrum channel can change, but the central frequency remains the same, and in elastic spectrum allocation, both the spectrum width and the central frequency can change over time [32].

### C. TRAFFIC PREDICTION FOR NETWORK OPTIMIZATION

Recently, machine learning techniques for optical networking have been attracting the attention of researchers [4], [5]. In particular, various traffic prediction methods, from statistical, including autoregressive integrated moving average (ARIMA), to machine learning, including artificial neural networks (ANNs), have been proposed [38], [39]. Moreover, data stream mining techniques were explored for practical traffic prediction in a long-term perspective [40].

Furthermore, alongside traditional regression models of forecasting exact bit values, classification approaches for predicting traffic levels are considered [41]. Recent research works have demonstrated how prior knowledge about future traffic volumes from prediction models benefits routing algorithms and decreases blocking probability. In particular, traffic prediction can be used to calculate the maximum expected bitrate between each pair of nodes in a given period and use this number for link congestion estimation to distribute the traffic evenly in the network [12]. Furthermore, graph neural network models are considered to predict traffic load on network links and enable considerable bandwidth blocking probability reduction [14]. Moreover, deep learning traffic prediction models allow for proactive and dynamic allocation of network resources, thus enabling considerable capacity savings and over-provisioning decrease at the cost of a marginal traffic loss [42]. Finally, traffic prediction can be used for periodic virtual network reallocations and result in notable savings in transponder usage [13].

Traditionally, dedicated prediction models can be developed for traffic between each source-destination pair, traffic class, or for each connection request (e.g., [18], [43], [44], [45]). Moreover, the traffic load on all network links can be predicted using a graph neural network model (e.g., [14], [46], [47]). Finally, the advantages of data aggregation and clustering for simultaneous traffic prediction between all pairs of nodes in large topologies have been studied in our previous work [48]. However, to the best of our knowledge, aggregated prediction models for backbone networks considering various reallocation periods have not been proposed in the existing literature.

## III. NETWORK AND TRAFFIC MODEL

In this Section, we first outline our network model and then provide the details of our time-varying traffic model.

### A. NETWORK MODEL

The considered network is a translucent SS-FON using a flexible spectrum grid of 12.5 GHz frequency slots. The network nodes are equipped with coherent and reconfigurable transceivers that support various modulation formats, namely, BPSK, QPSK, 8-QAM, and 16-QAM. In this work, we assume that the SS-FON is composed of links built as a bundle of single-mode fibers (SMFs). However, the network model and the optimization algorithm presented below can be adapted to apply other types of SDM fibers, e.g., few-mode fibers (FMFs) or multi-core fibers (MCFs).

The main assumptions are analogous to our previous papers focused on SS-FONs [49], [50]. In more detail, a transceiver supports transmission of a signal on an optical carrier (OC) that consists of three adjacent frequency slots (i.e., the OC is 37.5 GHz wide). The bit-rate supported by a single transceiver is a function of the modulation format selected for a particular lightpath. If the request's bit-rate exceeds the maximum capacity of a single transceiver under

the selected modulation format, the request is established using several carriers, transmitted within one spectral super-channel (SCh) with the same modulation format, and allocated an adequate number of adjacent frequency slots. Each SCh is separated from the adjacent SCh by a 12.5 GHz guard-band. Table 1 shows the transmission reach and supported bit-rate for modulation formats analyzed in this paper and used in simulation experiments [51].

**TABLE 1. Modulation formats - transmission reach and supported bit-rate.**

	BPSK	QPSK	8-QAM	16-QAM
Transmission reach [km]	6300	3500	1200	600
Bit-rate [Gbps]	50	100	150	200

Since the considered optical network is translucent, signal regeneration is supported at some transitional nodes of the lightpath. To this end, transceivers connected in a back-to-back (B2B) configuration are utilized [52]. In consequence, in the considered network, transceivers are used for two purposes: transmitting/receiving (add/drop) of the signal at the origin/destination nodes and regeneration of the signal at selected transitional nodes. Due to the B2B regeneration approach, instead of the routing, spatial mode, and spectrum (RSSA) optimization problem, a more demanding problem is to be addressed that accounts for transceiver assignment to end nodes of the lightpath and to the transitional nodes with regeneration. Thus, each lightpath can be divided into transparent segments, and each request can be realized in the network with various regeneration options (i.e., various nodes can be implemented with regeneration). In this paper, we name these options *configurations*. For each transparent segment of a particular configuration, the most efficient modulation format is selected according to the segment length and maximum transmission reach of the applied modulation format. It should be stressed that a key issue in B2B regeneration is that transceivers are used for add/drop of the signal at the origin/destination nodes and regeneration of the signal at transitional nodes. What is more, B2B regeneration allows for spectrum conversion (continuity constraints relaxation) in the node, i.e., after leaving the node, the spectral super-channel assigned to the lightpath can occupy a different part of the spectrum than the one that entered the node.

## B. TRAFFIC MODEL

Similarly to the traffic model in [53], traffic features are based on time-varying trends extracted from real-world measurements from Seattle Internet Exchange Point (SIX) available in [3]. The idea is to obtain a generalized shape of the traffic distribution over 24 hours or on a large scale throughout the week, which will be used more as a base shape for generating changes in time. For the sake of our custom traffic generator, we assume that all expected traffic can be divided into multiple services (each with an assigned share)

according to [54] such as: Internet videos, which occupy 51% of the total traffic; IP VoD with 22% share; web data with 18% share; file sharing with 8% share; and gaming with 1% share. Each of these services is characterized by its own properties, such as different stochastic processes with individual parameters, influencing and shaping traffic generation. These features are essentially formed by combining three basic stochastic processes, namely the Poisson Process (PP), the Poisson Pareto Burst (PPBP) Process, and constant traffic (CT) with uniform random offset distribution. In addition to the widely used Poisson process, PPBP was used to better model long-tail traffic modeling and constant traffic to mimic the base traffic, which is not necessarily influenced by time. For the stochastic processes mentioned above, their combinations are assigned to each service. For the Internet video service, the set of PPBP, CT, and two CTs is chosen. Next, the IP VoD consists of PP, and the web data traffic is generated by two PPs. The file sharing and gaming services are represented by a single CT each. This differentiation aims to capture the varied characteristics of Internet traffic.

Another feature of our traffic generator is that the created time-varying traffic can be adjusted to the parameters of a given topology. This is performed by distributing requests among the nodes of the given topology based on some popularity metric. The first option, commonly employed as the default traffic model in similar papers, entails evenly distributing requests among all nodes to ensure equal traffic between each pair of nodes (this scenario is referred to as *normal* traffic). The second option takes inspiration from the multi-variable gravity model proposed in [55], i.e., the traffic depends on the distance between nodes. In more detail, the total amount of traffic from one node to all others remains the same as in the previous scenario uniform, however, the traffic for each pair is inversely proportional to the distance between them (this scenario is referred to as *distance* traffic).

There is also an option to apply timezones for the traffic inside the given topology with modeled time-varying traffic, so the intensity across the day could be different between different nodes representing cities, according to given settings (e.g., peak hour between Seattle and Los Angeles can be different than between New York and San Francisco).

## IV. ALGORITHMS

The following Section describes the main components of the allocation algorithm proposed to solve the problem of periodic allocation of lightpaths in SS-FON based on the incoming traffic. The input for the problem consists of an SS-FON network and time-varying traffic. The SS-FON network is characterized by its topology, along with the specified quantity of spectrum resources (spectrum slots) and transceivers located at network nodes. Moreover, the network is able to perform the B2B regeneration as described in Section III-A. In turn, the time-varying traffic is defined for each

pair of nodes that exchange information. The optimization problem consists of periodic solving of the RSSA problem. The primary objective is to allocate traffic requests and periodically reallocate the network in response to changes in traffic. The goal is to minimize the bandwidth blocking probability (BBP), which is calculated as the volume of rejected traffic divided by the volume of the total traffic offered to the network.

## A. OVERVIEW

In general, our algorithm consists of three main components. The first is the periodic allocation, which controls how often the allocation is made. This approach adjusts the allocation of resources for each pair of nodes according to the traffic required (or predicted) in the next allocation period. This approach is a state-of-the-art method used for optimization of time-varying traffic in optical networks, e.g., [56] and [57]. The method, along with examples, is presented in Section IV-B. The second component is an order of processing each of the nodes' pairs that steers the way of saturating the network with resource allocation. The inspiration for using this approach comes from effective heuristic methods developed for the routing and spectrum allocation problem in EONs [58], [59], [60]. The rationale for the method and several proposed approaches are described in Section IV-C. The third component is the ARBR (Adaptive Routing with Back-to-Back Regeneration) method [49], which controls the routing and spectrum allocation for a lightpath, which is used to provision the traffic for a given pair of nodes to minimize the bandwidth blocking. According to the results reported in [49] and [61], the ARBR algorithm outperforms other reference methods in dynamic optimization of SS-FONs. A detailed description of the ARBR method is presented in Section IV-D.

The combination of the methods mentioned above results in different capacities and provides one of the key contributions of this work. The selection of these methods that are adjusted to the network model and the traffic provided gives a significant improvement in terms of the traffic served without the need for modification or increasing the number of resources available in the network.

The key concept of the proposed allocation algorithm is the *reallocation period* (RP). In more detail, due to the time-varying traffic considered in our work, the time scale is divided into smaller periods for which the new allocation of resources is performed, so the usage of those would be more precisely adjusted to current requirements in the given time period. More details about this part of the algorithm can be found in Section IV-B.

Another key part of the algorithm is the information about the incoming traffic in each RP, which is utilized during the allocation process. As a baseline, we assume the ideal 100% prediction to benchmark and configure the proper algorithm settings. Then, we use the traffic prediction models, which are described in Section V.

The general flow of the algorithm is shown in Fig. 1, which presents each of the described parts and how they interconnect with each other.

This article can be treated as a continuation and extension of the work begun in [50], but also as a separate set of new ideas that connect to concepts already researched. Work [50] introduced the concept of a reallocation period and briefly tested it in a smaller set of scenarios. In contrast to the above work, this article takes into account more topologies, types of traffic, routing algorithms, and different types of reallocation periods. Also, in this paper, we introduce the concept of configuration sorting methods other than the previously used *index\_asc*, which is a reference method in the simulations. On top of that, all those concepts are combined, giving a new method for managing network resources for time-varying traffic in SS-FONs. The last difference when compared to [50] is that in this work, we use the traffic prediction models so as to mimic the complete real-world scenario.

## B. PERIODIC REALLOCATION

The allocation process is the process of reserving the number of available resources (spectrum and transceivers). To maximize the amount of served traffic and to minimize the blocked traffic, our proposed allocation algorithm sets up lightpaths periodically to adapt to changing traffic over time. The RP occurs at a certain interval, with all resources released to create a new configuration for each pair of nodes, potentially resulting in a different selection of the lightpath (in terms of routing paths and spectrum). Since the traffic is to be established between each pair of nodes, the algorithm is divided into individual runs for each pair of nodes. In each step, the goal is to find a lightpath configuration that meets the needed traffic while permitting effective resource management for other node pairs. For instance, a basic approach could be a method where the pairs are analyzed in a lexicographic order, though this order can be altered and can cause a different blocking for the same amount of traffic and available network resources. This is discussed in Section IV-C.

Since the main goal of our research is to provide an overall verification of the concept of periodic reallocations to take advantage of the specific characteristics of time-varying traffic, we do not address the reconfiguration time of resources. However, in our future plans we want to address this issue and develop an optimization framework for a hit-less reallocation scheme that will account for time constraints of the network reconfiguration process.

It should be underlined that the reallocation period of 24 hours (RP = 24 hours) is our reference scenario, called *one-time allocation approach*. In more detail, the single allocation approach assumes that there is no reallocation and the network does not adjust to time-varying traffic and does not utilize the fact that the traffic is different throughout the day. Comparison of our optimization approach allowing

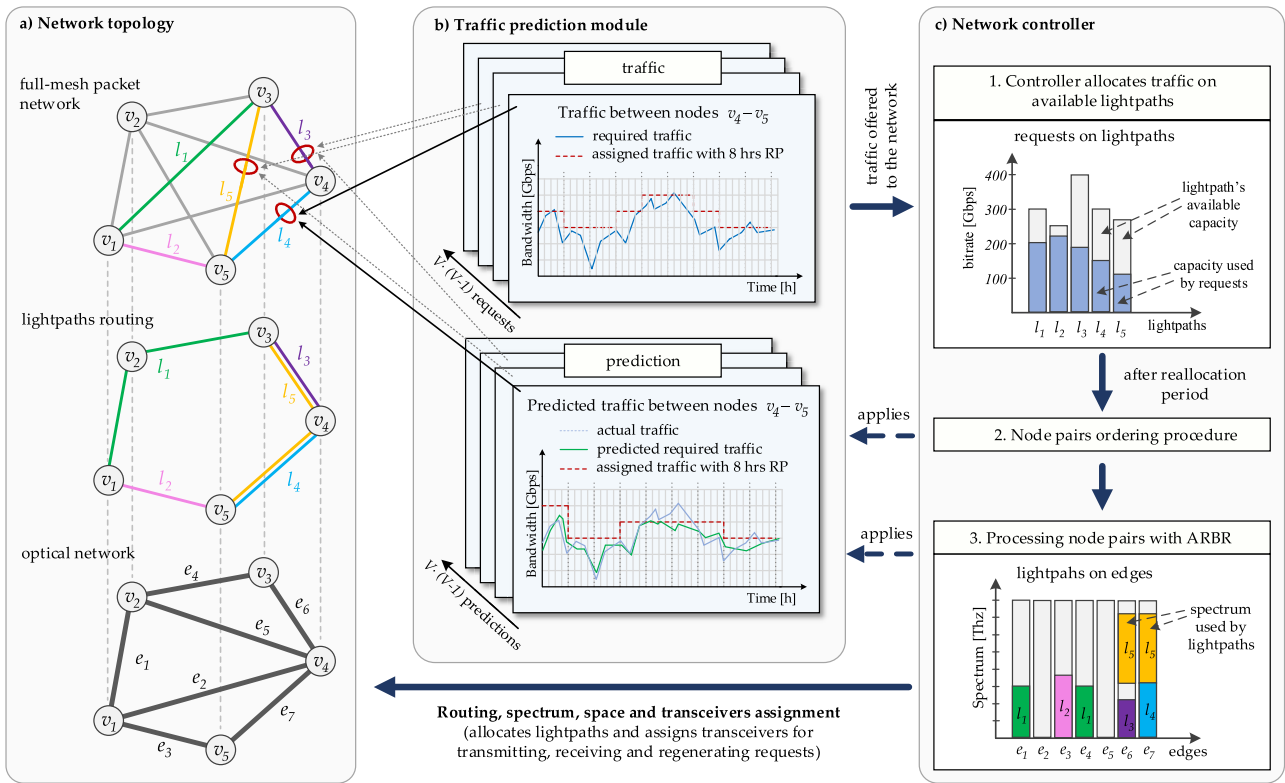


FIGURE 1. Flow diagram of the proposed algorithm.

periodic reallocation against the single allocation approach and evaluation of the potential benefits in terms of our is one of the main goals of this paper.

We present the following example to illustrate the advantage of frequent reallocation compared to just one allocation allowed for a given amount of time. For instance, a certain number of frequency slots must be reserved to fulfill the traffic requirement for a given pair of nodes. Fig. 2 depicts a request for traffic that varies over time for a given pair (blue line). It can be seen that since the required bit-rate changes over time, the number of frequency slots needed also varies.

In the case of the one-time allocation approach, in which only one resource allocation is done per day (purple dotted line, RP = 24 hours), continuously reserving 400 Gbps bandwidth is unnecessary. In the given example, only 4 hours out of the 24 require 400 Gbps bit-rate. Reallocations with lower RPs (represented by green and red dotted lines) which fit the request in the allotted time permit the efficient utilization of the free spectrum resources on lightpaths for the remaining pairs of nodes. This example shows that frequent reallocations are more efficient in making use of available resources and can improve the capacity of the network since further allocation for other pairs of nodes will be needed, and potentially also with the use of gained resources. We assume that the value of the RP parameter is constant throughout the simulation.

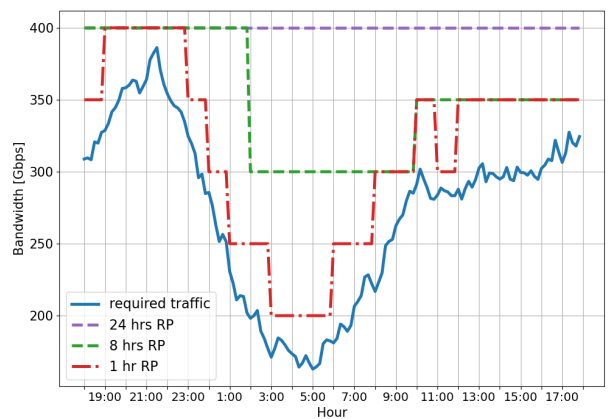


FIGURE 2. Reserved bandwidth for different RPs depending on given required traffic.

### C. ORDERS

As described in Section IV-D, the cost function of each configuration for a pair of nodes is calculated separately and sequentially since the state of the network taken into account depends on previously selected configurations. With that in mind, the total capacity of the network may vary for different orders of processing of pairs of nodes. On the basis of that, we take into account various orders of processing, which can be divided into three main groups.

The first type of order is based on the distance between each pair of nodes, which corresponds to the length of the shortest path between those and is measured in kilometers. With these values, the list of node pairs to be processed by the ARBR algorithm is sorted. In this case, we select two types of orders, namely, ordering by distance in ascending order and by distance in descending order, denoted by *distance\_asc* and *distance\_dsc*, respectively. This approach assumes that the best way to allocate resources is to start with the node pairs located relatively close to each other so that the subsequent heuristic computation is more suited to the state of the system. In contrast, it could be preferable to start with the longest distances between the analyzed node pair so that the most demanding configurations are chosen first. In essence, these methods focus on the resources that must be assigned in relation to the distance, such as the number of hops or the highest modulation format available.

The second considered type is based on lexicographic order, that is, it sorts pairs of nodes based on the assigned number of source and destination nodes. From this approach, we distinguish two methods of sorting: by index in ascending order (denoted by *index\_asc*) and by index in descending order (denoted by *index\_dsc*). These are the benchmark approaches with no real-world rationale, but rather to compare to other methods, as it is a natural way of listing the paths in a network. The *index\_asc* sorting method is also the only one used in our previous work [50].

The third group is the order by the amount of predicted required traffic in the next RP for each pair of nodes. There are also two possibilities here, namely, ordering from the pair of nodes with the highest required bandwidth to the one with the lowest, denoted by *traffic\_dsc*. The other ranges from lowest to highest, denoted by *traffic\_asc*. The rationale behind these is that maybe it is better to allocate the highest requested bandwidth initially so to avoid the blockage for those as a priority. Alternatively, maybe it would be better to handle the smallest requests, so with a saturated system, the ARBR algorithm would be better suited for those.

#### D. ARBR

In this Section, we describe the ARBR algorithm that was proposed for the first time in [49] and then applied to various optimization problems in SS-FONs with B2B regeneration, for example, [61], [62]. The ARBR algorithm is used for dynamic routing in SS-FON, and the goal of this algorithm is to try to establish a request in order to minimize the blocking.

As we consider time-varying traffic and periodic reallocations during which the resources can be reassigned, the lifetime of each request for the ARBR algorithm is equal to the reallocation period (starting at the same timestamp). Between each pair of nodes, there is requested bandwidth changing in time according to the traffic model described in Section III-B. As the overall bandwidth is composed of multiple services, traffic between each pair of nodes can be treated by the ARBR either as a large single request with the

bit-rate equal to the accumulated bandwidth or divided into an arbitrary number of smaller requests that can accommodate the same total capacity if needed.

We assume that the SS-FON is modeled as a graph  $G = (V, E)$ , where  $V$  denotes a set of optical nodes and  $E$  denotes a set of fiber links composed as a bundle of  $K$  SMFs. In each SMF  $k \in K$  the optical frequency spectrum is organized as a set  $S = \{s_1, s_2, \dots, s_{|S|}\}$  of 12.5 GHz frequency slots. The available modulation formats are denoted as a set  $M = \{m_1, m_2, \dots, m_{|M|}\}$ . Each modulation format  $m \in M$  is described by a certain transmission reach and spectral efficiency. A modulation format  $m \in M$  provides the transmission of a bit-rate  $g(m)$  on a single carrier. Using the data from the traffic prediction model (described in Section V), a traffic request  $d$  is assigned with a bit-rate  $h(d)$  to be transmitted in the network using a lightpath established on a route  $p$  connecting the request's end nodes and going through a set of intermediate nodes  $V(p) \subseteq V$ . For each request  $d$ , a set  $P(d)$  of candidate routing paths is available, created using the k-shortest path algorithm. The set  $R(p)$  contains allowable B2B regeneration options for path  $p$ . A regeneration option  $r \in R(p)$  is described by a subset  $V(r) \subseteq V(p)$  of regeneration points, which means that the path  $p$  is divided into a set of consecutive path segments  $r = \{q_1, q_2, \dots, q_{|r|}\}$  and the path segments have end nodes in regeneration points  $V(r)$ . The best (in terms of the spectral efficiency) modulation format  $m(q) \in M$  is chosen for the SCh using path segment  $q \in r$ , guaranteeing that the transmission reach of  $m(q)$  exceeds the length of the path segment  $q$ . Let  $n(q, d)$  denote the number of OCs required for path segment  $q$  of request  $d$ . Note that  $n(q, d)$  is a function of the carried bit-rate and selected modulation format, that is,  $n(q, d) = \lceil h(d)/g(m(q)) \rceil$ . In consequence, the width (number of required frequency slots) of the path segment  $q$  in request  $d$  is defined as  $c(q, d) = 3n(q, d) + 1$ , since – according to the network model described in Section III-A – every OC includes three frequency slots and one additional frequency slot applied as a guard-band to isolate neighboring SChs. Finally, notice that the number of transceivers assigned to the request  $d$  on the path segment  $q$  corresponds to  $n(q, d)$  since each OC is generated/received using a single transceiver.

Now, we introduce some additional notation related to the concept of configuration introduced in Section III-A. Let  $\pi = (p, r)$  define a configuration where  $p$  denotes a routing path and  $r$  denotes a regeneration option (i.e., a division of the path  $p$  into path segments). Moreover, we assume that  $r(\pi)$  and  $p(\pi)$  denote a regeneration option and path of configuration  $\pi$ , respectively. Finally, let  $\Pi(d)$  denote a set of configurations available for request  $d$ .

Next, we focus on the definition of a metric used to measure the quality of various configurations for a request. Let  $FS(\pi, d) = \sum_{q \in r(\pi)} c(q, d)l(q)$  denote the total number of frequency slots necessary to establish request  $d$  using configuration  $\pi$ , where  $l(q)$  defines the number of links (hops) of the path segment  $q$ . It should be stressed



that  $FS(\pi, d)$  estimates the amount of spectrum resources required to establish request  $d$  on configuration  $\pi$ . In more detail,  $FS(\pi, d)$  counts frequency slots in all links applied to realize configurations  $\pi$  necessary to provide the request  $d$ . In an analogous way, let  $TR(\pi, d) = \sum_{q \in r(\pi)} t(q, d)$  denote the number of transceivers necessary to establish request  $d$  using configuration  $\pi$ .

Let  $c^{static}(\pi, d) = FS(\pi, d) + \frac{FS^{ALL}}{TR^{ALL}} TR(\pi, d)$  denote a metric assigned to the configuration  $\pi$  for the request  $d$ , where  $FS^{ALL}$  and  $TR^{ALL}$  denote the total number of frequency slots and transceivers available in the network, respectively. The rationale behind metric  $c^{static}(\pi, d)$  is to measure how much optical network resources (namely, spectrum and transceivers) are necessary to establish request  $d$  using configuration  $\pi$ . In the definition of  $c^{static}(\pi, d)$ , we apply  $\frac{FS^{ALL}}{TR^{ALL}}$  to ensure a similar influence of both types of resources (i.e., spectrum and transceivers).

Nevertheless, it should be noted that the metric  $c^{static}(\pi, d)$  measures only the static usage of resources in the network and does not refer to the dynamic traffic scenario. In more detail, in the dynamic traffic scenario, the usage of network resources (i.e., spectrum and transceivers) varies over time due to the dynamic allocation of resources to new requests arriving to the network and the deallocation of resources used by requests that are released from the network. Moreover, using purely the  $c^{static}(\pi, d)$  metric can trigger a scenario when requests are tried to be provisioned on congested links/nodes, and, in consequence, the requests are rejected due to the lack of spectrum/transceivers. To address this issue, we formulate a second metric that accounts for the dynamic traffic scenario  $c^{dynamic}(\pi, d) = MLU(\pi) + MNU(\pi)$ . Note that  $MLU(\pi)$  estimates a maximum link utilization considering all links included in configuration  $\pi$ . Furthermore,  $MNU(\pi)$  estimates the maximum node utilization in terms of used transceivers, considering all nodes included in configuration  $\pi$ .  $MLU(\pi)$  and  $MNU(\pi)$  metrics are computed as proposed in [63], i.e., for 0 – 10% utilization the metric is equal to 10, for 11 – 20% utilization is equal to 20, ..., for 91 – 100% utilization is equal to 100. Finally, combining the metrics  $c^{static}(\pi, d)$  and  $c^{dynamic}(\pi, d)$ , we are able to formulate the metric  $c^{adaptive}(\pi, d)$  that is used to measure the quality of the configuration  $\pi$  for requests  $d$ :

$$c^{adaptive}(\pi, d) = (1 - \alpha)c^{static}(\pi, d) + \alpha c^{dynamic}(\pi, d),$$

where  $\alpha$  is a tuning parameter applied to tune the impact of static and dynamic metrics.

The workflow of the ARBR algorithm is as follows. By processing the predicted traffic from the given prediction model and iterating over each traffic request  $d$ , for every configuration  $\pi \in \Pi(d)$  metric  $c^{dynamic}(\pi, d)$  is calculated accounting for the current situation in the network in terms of spectrum and transceiver utilization. Next, all configurations in  $\Pi(d)$  are processed in increasing order according to metric  $c^{dynamic}(\pi, d)$ . In more detail, it is checked if the request  $d$  can be provisioned in the network using the currently analyzed configuration  $\pi$ . If possible,

the request  $d$  is allocated on configuration  $\pi$ , and the algorithm stops. When none of the configurations allows provisioning the request, the analyzed request is rejected. Note that for spectrum allocation, the ARBR algorithm uses the spectral first-fit spectrum allocation method. To speed up the ARBR algorithm, allowable configurations for every pair of nodes are precomputed, and thus it is not required to compute configurations when a new request is to be processed.

The computational complexity of the ARBR algorithm run for a single request  $d$  is a result of three main elements. First, the link and node metrics are to be computed to find the value of metric  $c^{dynamic}(\pi, d)$  for each configuration  $\pi \in \Pi(d)$ . This operation has complexity of  $O(|V| + |S| |K| |E|)$ , where  $|V|$  denotes the number of nodes,  $|S|$  denotes the number of frequency slots,  $|K|$  denotes the number of SMFs,  $|E|$  denotes the number of links. The second element is due to the fact that all configurations are sorted in increasing order of metric  $c^{dynamic}(\pi, d)$ . Complexity of this operation is  $O(|\Pi(d)| \log(|\Pi(d)|))$ , where  $|\Pi(d)|$  denotes the number of configurations available for request  $d$ . The last element is responsible for processing all configurations to check if request  $d$  can be established using a particular configuration. Complexity of this operation can be estimated as  $O(|\Pi(d)| |S| |K| |E|)$ . Note that for each analyzed configuration the first-fit spectrum allocation method is run having the complexity of  $O(|S| |K| |E|)$ .

In this work, we consider two types of ARBR algorithm. The first uses  $\alpha = 0.8$  and is denoted in simulations by *ARBR* (the italics refer to a particular implementation of ARBR applied in the simulations). The chosen value of the  $\alpha$  factor is based on the algorithm tuning research in [49]. For the second case, we use  $\alpha = 0$  and denote it by *ARBR\_static*. The latter can be described as the ARBR algorithm with only the static part and is chosen because of its simplicity compared to the full approach and as a reference to see the gain in terms of proper configuration selection. For more details on the ARBR algorithm, please refer to [49].

## E. DISCUSSION

In this section, we discuss the proposed optimization framework. In more detail, we report scalability of the method and present some limitations. Moreover, we briefly highlight potential modifications and adaptations for other scenarios.

The complexity analysis presented in previous Section indicates that the main element of the optimization framework, i.e., ARBR algorithm, has polynomial complexity, what provides scalability of the proposed solution in larger, more complex network topologies. An important parameter influencing the complexity is the number of configurations ( $|\Pi(d)|$ ). However, this parameter can be tuned according to the needs and expected scalability. In more detail, the number of configurations is a function of the number of candidate shortest routing paths and the number of B2B regeneration options. In this work, we use 5 candidate

shortest paths. However, this parameter can be tuned for the purpose of the scalability. In a similar way, the number of B2B regeneration options can be reduced. Other elements of the proposed optimization framework also provide good scalability and can be used for networks of various size.

The computational requirements of the proposed resource allocation heuristics exhibit variation dependent on the predicted traffic volume, network size, and available resource quantity (including transceivers at topology nodes and cores on topology arcs). On a single CPU with a clock speed of 3.8 GHz, the execution time ranges from 1.77 to 4.96 seconds per one reallocation period, with an average value of 2.93 seconds.

It is worthy to underline, that the proposed optimization framework can be adapted to various types of hardware. To run numerical experiments, we made some assumptions on the applied hardware (see Section III-A). However, the developed algorithms (including the ARBR method) can be modified to work with other models of transceivers with different values of the key parameters concerning the supported modulation formats, transmission reach, number of used spectrum slots. The proposed solution can be easily extended to use either vendor specific connection planning tools or by using analytical or ML-based models in disaggregated optical networks to assure sufficient connection's quality of transmission.

It should be noted that this work is a preliminary research with the main goal to explore potential benefits of using dedicated strategies for leveraging the unique characteristics of time-varying network traffic in translucent SS-FONs. In operating network, periodic reconfiguration of optical connections can result in connections downtime. End-to-end optical path reconfiguration time can be on the order of several hundred milliseconds causing transmission loss [64]. However, we may expect that the reconfiguration time will be decreased in the future optical networks [65]. In this work, to reduce complexity and the scope of research, we made a simplification assumption that the time required for the network reconfiguration is very small. In consequence, the resources (i.e., transceivers and spectrum) used by lightpaths in the previous reallocation period are available for provisioning of new lightpaths in the next reallocation period. However, we would like to underline that the developed optimization framework and obtained results can be adapted for the hit-less reallocation approach that addresses more detailed constraints of the network reconfiguration process. In more detail, to account for a longer time required for the network reconfiguration, the optimization framework can be modified to change the moment when resources of lightpaths of the previous reallocation period are released. In particular, the new lightpaths are provisioned in the network before the resources of previous lightpaths are released. To facilitate the reallocation process, the optimization framework can reallocate only a fraction of all requests in a given moment and thus reduce the negative impact of overlapping of previous and new lightpaths.

Moreover, the proposed optimization approach can be easily enhanced to address network resilience and protect the network against potential failures. For this purpose, each traffic request in the network should be assigned two lightpaths using a pair of link-disjoint paths, which would protect against a single link failure. The only element of the proposed optimization framework that needs to be modified is the routing, spectrum, and space assignment algorithm. To this end the Adaptive Survivable Routing with Back-to-Back Regeneration (ASRB) algorithm proposed in [61] can be applied.

## V. TRAFFIC PREDICTION

In this article, we consider the time-varying traffic between all pairs of nodes in a backbone optical network. For instance, in a 28-node topology, that is, 756 separate time series. It poses a challenge to forecast such a large amount of targets simultaneously. A traditional approach uses dedicated prediction models for each network link, source-destination pair, traffic class, or for each connection request, e.g., [18], [43], [44], and [45]. However, graph neural network models are recently gaining popularity for predicting the traffic in the whole network at once, e.g., [14], [46], and [47]. Nevertheless, such models are designed rather for forecasting the utilization of specific links than for more versatile predictions of traffic between node pairs. In the scenarios considered in the literature, the network snapshot graphs analyzed by the ML algorithms have less than 100 edges, as they only contain actual links in the underlying backbone network architecture. Note that such a framework infers some routing algorithm placing individual connection requests into specific lightpaths. More generic information about future traffic between node pairs enables the creation of a more informed routing algorithm that can adapt its decisions and thus place more traffic into the network [12]. Furthermore, a graph where all nodes are connected with each other has a very regular structure and therefore is not an ideal use case for graph neural networks [66]. On the contrary, training individual prediction models for each pair of nodes makes the task too complex for large network topologies.

The proposed traffic prediction model is inspired by our research in [67], where we showed how information about other types of traffic in the network improves the prediction quality of a single traffic type. Following this idea, we create a general, aggregated prediction model (*APM*), which uses multioutput regression for simultaneous forecasting of the traffic between all pairs of nodes. That way, we reduce the number of necessary models to only one. As an added bonus, since the relationships between targets are available to the model, multioutput regression methods are known to yield better predictive performance, in general, when compared to the single-output methods [68].

Following our idea from [67], the proposed *APM* uses additional temporal features created from past, highly correlated samples of each timeseries (traffic measurements between one pair of nodes). As also shown in [69], such

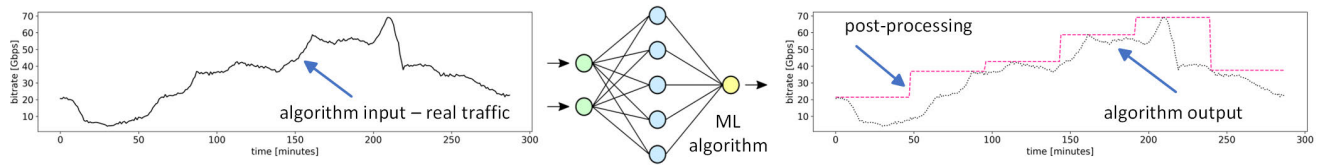


FIGURE 3. *APMpost* illustration.

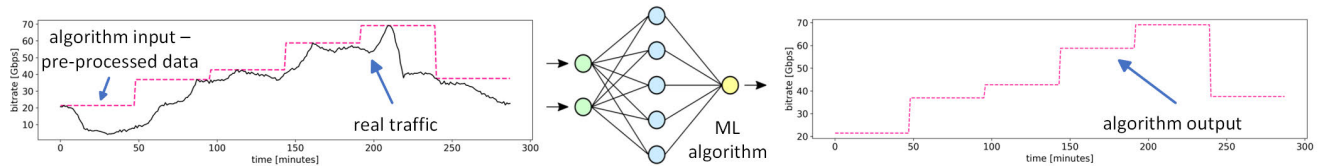


FIGURE 4. *APMpre* illustration.

features are very effective for traffic prediction, as they have the highest contribution in the model decision compared to other possible inputs. Furthermore, as shown in [40] and [70], models based on such features can successfully adapt to changing traffic patterns and unseen traffic types. Due to the varying forecast span (more details in the next paragraph), for each timeseries, we use two additional features: the amount of traffic measured a day and a week before the forecasted period. In turn, an aggregated multitarget model predicting 756 timeseries uses  $2 \cdot 756 = 1512$  features. Note that this is still a relatively small model compared to deep learning, where dramatically more parameters are needed; thus, the resulting models are much more complex [71].

We consider traffic forecasting a regression problem where exact bit values are predicted. However, the proposed routing algorithm employs the idea of RPs, where lightpaths are established, considering the maximum expected traffic in the next period. Nevertheless, as in real-world networks, the operator has access to more granular traffic measurements, which can be further used to train a more versatile prediction model. In this work, we wish to compare two proposed approaches. In the first one, called *APMpost*, the model is trained on one-minute-sampled traffic data and outputs a detailed minute-by-minute forecast for the coming period. Then, the maximum predicted traffic is extracted from the obtained forecast and passed to the routing algorithm. The idea behind this model is illustrated in Fig. 3. In the second approach, *APMpre*, the historical data is preprocessed by extracting maximum traffic values from each period and then training the model. In turn, the created model outputs only one value, corresponding to the maximum traffic in the subsequent period. The idea behind this model is illustrated in Fig. 4. To the best of our knowledge, this is the first approach to propose traffic prediction methods for various RPs in the literature.

Note that our proposed *APM* is generic and thus can be used with any ML algorithm. In this work, our ML algorithm of choice is linear regression (LR). As shown by the authors of a recent study [72], for optical-network-related tasks, the use

of LR can provide results of similar quality to deep learning techniques at a notable complexity decrease, following the green networking paradigm [73]. Similarly, in [40], the LR-based streaming approach outperformed various neural network models in long-term traffic prediction, and, in our previous analysis [67], LR achieved the lowest prediction errors across traffic types.

## VI. RESULTS

In this Section, we first give an overview of the simulation setup, then discuss the algorithm tuning. Finally, we dive into the details of the results we obtained.

### A. SIMULATION SETUP

For the experiment, we use two representative optical network topologies: Euro28 (28 nodes, 82 links, average link length of 625 km) and US26 (26 nodes, 84 links, average link length of 755 km) shown in Fig. 5 [60]. We use the network model described in III-A. We assume that each link in SS-FON is a bundle of 12 SMFs, where each SMF provides 320 frequency slots, each of 12.5 GHz width. Network nodes are equipped with the same number of coherent transceivers that operate at a fixed baud rate, where each transceiver transmits/receives an optical signal that occupies three frequency slots (i.e. 37.5 GHz). The total number of transceivers available in the network is 10 000, 15 000, or 20 000, which are evenly distributed for all nodes.

The main performance metric is *bandwidth blocking probability* (BBP), defined as the volume of rejected traffic divided by the volume of the whole traffic offered to the network. Furthermore, we use a metric called *accepted traffic* for 1% threshold of BBP. To obtain this metric, we simulate a particular scenario for various values of traffic load expressed to find the maximum traffic that can be provisioned in the network with a BBP of 1%, a commonly acceptable threshold for BBP.

The simulations were realized within the authors' custom software written in Python 3.11 programming language using the standard module along with *scipy*, *numpy*, *pandas*

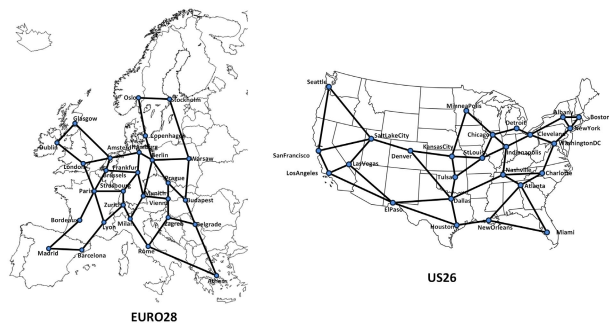


FIGURE 5. Tested network topologies.

third-party libraries. The computations were parallelized using the MPI protocol (each considered scenario occupied a single core, giving a total of 12 separate and independent runs at the same time).

The setup of the simulator depends on several control parameters. The consider topology defines the main parameters, i.e., the number of nodes, the number and lengths of links that connect them, and the overall number of pairs of nodes. In our simulator every pair of nodes is taken into account during the allocation process. Next parameters are the setting of resources in a given topology, such as the number of transceivers in each node and the number of SMFs at each link. For the setting of allocation procedure and the reallocation period duration, the routing algorithm and the method of ordering possible lightpath configurations for each pair of nodes are the key parameters. With the given time-varying traffic that is quantified into chunks of required traffic for each pair of nodes, the simulator iterates over each pair of nodes (in order defined by the sorting method) and tries to allocate resources that would provide a lightpath that would provision the required traffic load in given time range (defined by the reallocation period). If the required traffic could not be provisioned for a given pair of nodes, the simulator treats this traffic as a blocked traffic. At the end of the simulation, simulator based on the total blocked traffic and the with overall traffic computes the main performance metric of BBP. Moreover, the simulator collects other metrics such as number of used transceivers and used frequency slots.

**B. ALGORITHM TUNING**

The tuning stage was performed with the use of multiple scenarios that could point to the best combination of ARBR type and configuration sorting methods, that is:

- 2 topologies: Euro28 and US26.
- 4 types of traffic: *normal* and *distance*, with or without timezones applied.
- 2 routing algorithms: *ARBR* and *ARBR\_static*.
- 3 transceiver numbers: 10 000, 15 000 and 20 000.
- 2 reallocation periods: 15 minutes and 1 hour.
- 6 configuration sorting methods: *distance\_asc*, *distance\_dsc*, *index\_asc*, *index\_dsc*, *traffic\_asc*, and *traffic\_dsc*.

The total number of scenarios to investigate is 576. From these scenarios, the 12 main methods can be extracted, which are characterized by the type of routing algorithm and sorting methods. So, all of these 12 methods are tested against 48 scenarios which are grouped into four groups depending on the tested topology, namely Euro28 and US26, and tested traffic type, named as *distance* and *normal*, which are described in Section III-B.

Example methods' benchmarks for given scenarios are presented in Fig. 6 and 7 and show the performance of each method in terms of BBP for 24 hours depending on the given traffic. It can be seen that some methods perform noticeably better compared to others and can provide a 1% BBP for the higher required traffic. Recall that the reference method, used in [50], is the *ARBR index\_asc* and is the only such approach known to the authors.

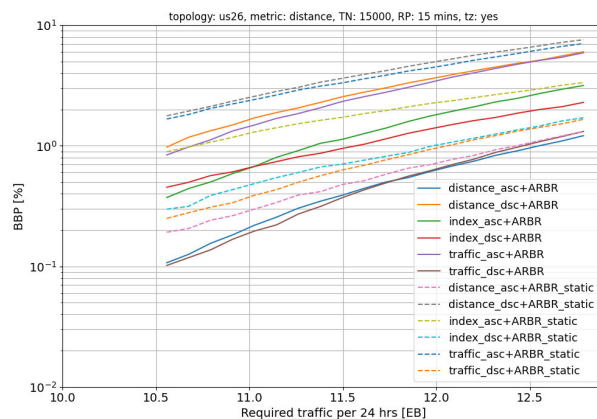


FIGURE 6. An example benchmark of methods for a test configuration consisting of US26 topology with 15 000 transceivers, 15 min RP for distance traffic with timezones.

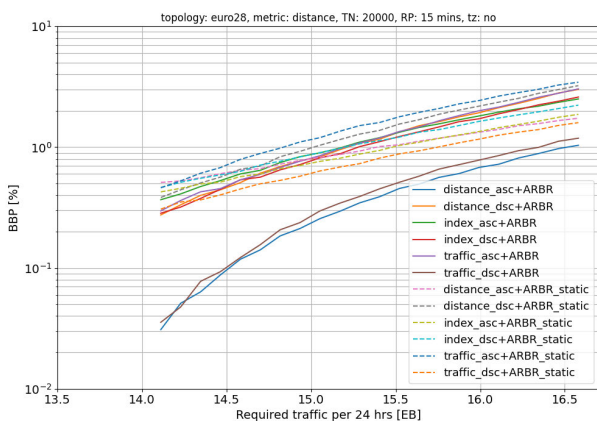


FIGURE 7. An example benchmark of methods for a test configuration consisting of Euro28 topology with 20 000 transceivers, 15 min RP for distance traffic without timezones.

Through multiple tuning simulations, for each scenario, the best method was found by comparing the highest, 24-hour accepted traffic with 1% BBP, and according to that amount of required traffic, the BBPs for other methods were

**TABLE 2.** Tuning for the Euro28 topology.

Sorter	Order	Traffic type: distance		Traffic type: normal		$\Sigma R1$	$\Sigma R2$
		$R1$	$R2$	$R1$	$R2$		
ARBR	<i>distance_asc</i>	4	0.18	0	0.00	4	0.18
ARBR	<i>distance_dsc</i>	120	31.30	76	12.30	196	43.61
ARBR	<i>index_asc</i>	64	12.98	55	9.13	119	22.11
ARBR	<i>index_dsc</i>	84	17.51	70	10.51	154	28.01
ARBR	<i>traffic_asc</i>	116	30.18	27	4.70	143	34.89
ARBR	<i>traffic_dsc</i>	20	2.75	37	6.14	57	8.89
ARBR_static	<i>distance_asc</i>	24	4.36	84	9.30	108	13.65
ARBR_static	<i>distance_dsc</i>	108	28.28	120	15.41	228	43.69
ARBR_static	<i>index_asc</i>	48	9.11	75	9.27	123	18.38
ARBR_static	<i>index_dsc</i>	68	12.76	108	13.83	176	26.59
ARBR_static	<i>traffic_asc</i>	112	29.08	53	8.86	165	37.93
ARBR_static	<i>traffic_dsc</i>	24	4.75	87	11.02	111	15.77

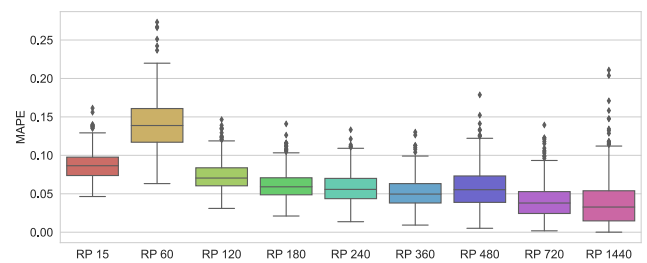
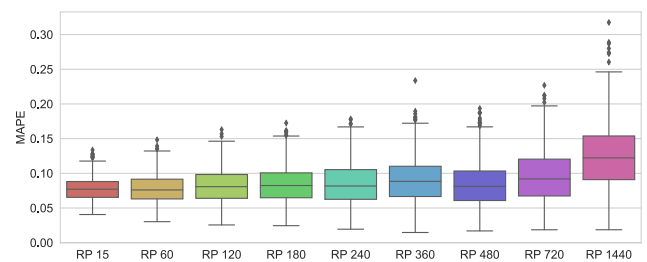
calculated. We propose two types of ranking methods. The first, denoted as  $R1$ , is to rank the methods for each scenario in the given group from 0 to 11, where 0 denotes the lowest BBP (that is, 1%) and 11 the highest. This means that the method which is the best for all scenarios in a given group would have a ranking  $R1 = 0$ , and similarly, the method which is the worst for all cases would have  $R1 = 132$  since there are 12 scenarios for each group. The other ranking method, denoted as  $R2$ , consists of assigning the difference in BBP of a given method and the BBP of the method with the lowest BBP. For example, if, for a given scenario, method A has 1% BBP (and has the lowest BBP from all methods for the given scenario) and method B has 7.8% BBP, then the ranking  $R2$  would equal 0 for method A, and 6.8 for method B, respectively.

Tables 2 and 3 show the tuning results for the Euro28 and US26 topologies, respectively. Results are grouped for the *distance* and *normal* metric (i.e., traffic type). The columns  $\Sigma R1$  and  $\Sigma R2$  are sums of  $R1$  and  $R2$  for both mentioned groups. As can be seen, for the Euro28 topology, the method *ARBR distance\_asc* outperforms other methods. For the US26 topology, the mentioned method is also the best. However, in this case, the method *ARBR traffic\_dsc* has close ranking results.

### C. TRAFFIC PREDICTION

To evaluate the quality of the proposed traffic prediction models, first, we use the *mean absolute percentage error* (MAPE), as it enables a direct comparison of the methods' performance on traffic timeseries differing vastly in volume. Moreover, it is a commonly used measure in the network traffic prediction problem (e.g., [73], [74]).

Fig. 8 and 9 present the MAPE distribution across considered 756 pairs of nodes in Euro28 topology for different RPs (given in minutes) for *APMpre* and *APMpost*, respectively. The prediction quality is prominent, with average MAPE values between 3-14%, depending on the model and RP.

**FIGURE 8.** MAPE distribution across pairs of nodes for different RPs for *APMpre*, Euro28 topology.**FIGURE 9.** MAPE distribution across pairs of nodes for different RPs for *APMpost*, Euro28 topology.

Interestingly, the prediction quality trends regarding different forecast horizons are quite the opposite between the models. For *APMpre*, the average prediction error decreases with the increase of the forecasted period, with a spike for the 60-minute forecast period. That is not the case for *APMpost*, where, on average, more accurate predictions were obtained for shorter time windows. To recall, *APMpre* is trained on preprocessed data, with the historical maximum traffic values from each period available directly to the model. On the contrary, *APMpost* outputs minute-by-minute forecasts, and the maximum traffic values for the predicted periods are extracted in post-processing. From a practical perspective, the detailed predictions of *APMpost* can be more versatile as they

TABLE 3. Tuning for the US26 topology.

Sorter	Order	Traffic type: distance		Traffic type: normal		$\Sigma R1$	$\Sigma R2$
		$R1$	$R2$	$R1$	$R2$		
ARBR	<i>distance_asc</i>	4	0.58	15	3.38	19	3.97
ARBR	<i>distance_dsc</i>	112	49.02	88	31.18	200	80.20
ARBR	<i>index_asc</i>	72	19.29	44	10.09	116	29.39
ARBR	<i>index_dsc</i>	60	13.92	78	16.91	138	30.84
ARBR	<i>traffic_asc</i>	96	46.57	15	2.63	111	49.20
ARBR	<i>traffic_dsc</i>	13	0.68	18	3.34	31	4.02
ARBR_static	<i>distance_asc</i>	19	2.18	44	12.07	63	14.25
ARBR_static	<i>distance_dsc</i>	132	61.45	128	53.50	260	114.95
ARBR_static	<i>index_asc</i>	84	22.80	104	34.42	188	57.22
ARBR_static	<i>index_dsc</i>	43	6.31	62	15.34	105	21.65
ARBR_static	<i>traffic_asc</i>	116	54.11	97	29.52	213	83.63
ARBR_static	<i>traffic_dsc</i>	41	5.12	99	30.38	140	35.50

allow the operator to calculate the maximum expected traffic in any chosen horizon on-the-fly.

As our recent studies show, the choice of a traffic prediction model can vary quite significantly between metrics [40], [75]. For that reason, we further expand our evaluation. In Fig. 10, we report the ratio of forecasted timeseries that had more accurate predictions according to four metrics for considered RPs. Such presentation enables visual comparison of error measures dependent on the traffic volume and thus not directly comparable between traffic in different pairs of nodes. We consider the aforementioned MAPE, two other standard regression metrics: *mean squared error* (MSE), *coefficient of determination* (R2), and a recently proposed *allocation outside blocking threshold* (AOBT) [40], [75]. The latter is a parameterized measure that links the problem of traffic forecasting with *bandwidth blocking probability* (BBP). In this paper, we use equal slope parameters of 2 and an acceptable blocking threshold of 1%. For more information about the AOBT, we refer to [40], [75].

The differences between the evaluation of different metrics are apparent in Fig. 10. Nevertheless, some common trends emerge between them. In particular, for almost all pairs of nodes, for RP of 60 minutes, more accurate predictions were given by *APMpost*, which is also true for RP of 15 minutes in most cases. However, for larger RPs, *APMpre* provided better forecasts. For RPs of 720 minutes and 1440 minutes (24 hours), almost all timeseries were predicted more precisely with this model. It is the most notable for RP = 1440 minutes using the R2 metric – for all pairs of nodes, *APMpre* delivered closer to perfect predictions. In summary, from the ML point of view, *APMpost* is a better choice for smaller RPs, while *APMpre* should be used for larger RPs.

As illustrated above, the proposed traffic prediction model provides satisfactory forecast quality across network node pairs. However, ML models tend to minimize standard metrics to obtain the lowest-possible errors without considering

the real-world application [40], [75]. The best-overall regression function is thus sought to balance over- and under-estimations. In turn, even for light traffic load, due to little traffic underestimation, insufficient resources can be prepared for the coming requests causing infeasible solutions and blocking, despite still having free capacity within the network. Therefore, as in related literature (e.g., [76]), the algorithm considers the predicted traffic values with an additional 10% overhead to minimize the mentioned unnecessary blocking when the resources are still available in the network.

#### D. EVALUATION OF VARIOUS SCENARIOS

As shown in Section VI-B, in our tuning tests, the method *ARBR distance\_asc* performed the best. In this Section, we evaluate a set of scenarios which test the performance of that method for more RPs in terms of BBP and resource usage.

This stage of numerical experiments consists of the following scenarios:

- 2 topologies: Euro28 and US26.
- 4 types of traffic: *normal* and *distance*, with or without timezones applied.
- 3 transceiver numbers: 10 000, 15 000 and 20 000.
- 9 reallocation periods: 15 minutes, 1 hour, 2, 3, 4, 6, 8, 12, 24 hours.
- 1 algorithm method: *ARBR distance\_asc*, that is, *ARBR* routing algorithm with a configuration sorting method *distance\_asc*.

The total number of scenarios to investigate is 216. To recall, the one-time allocation approach with reallocation period of 24 hours (RP = 24 hours) is as a reference scenario used to verify what are the gains of using our optimization framework that adjusts the network configuration to time-varying traffic by utilizing the fact that the traffic is different throughout the day. Fig. 11 presents two example sets of scenarios for which the trends of changes in used resources

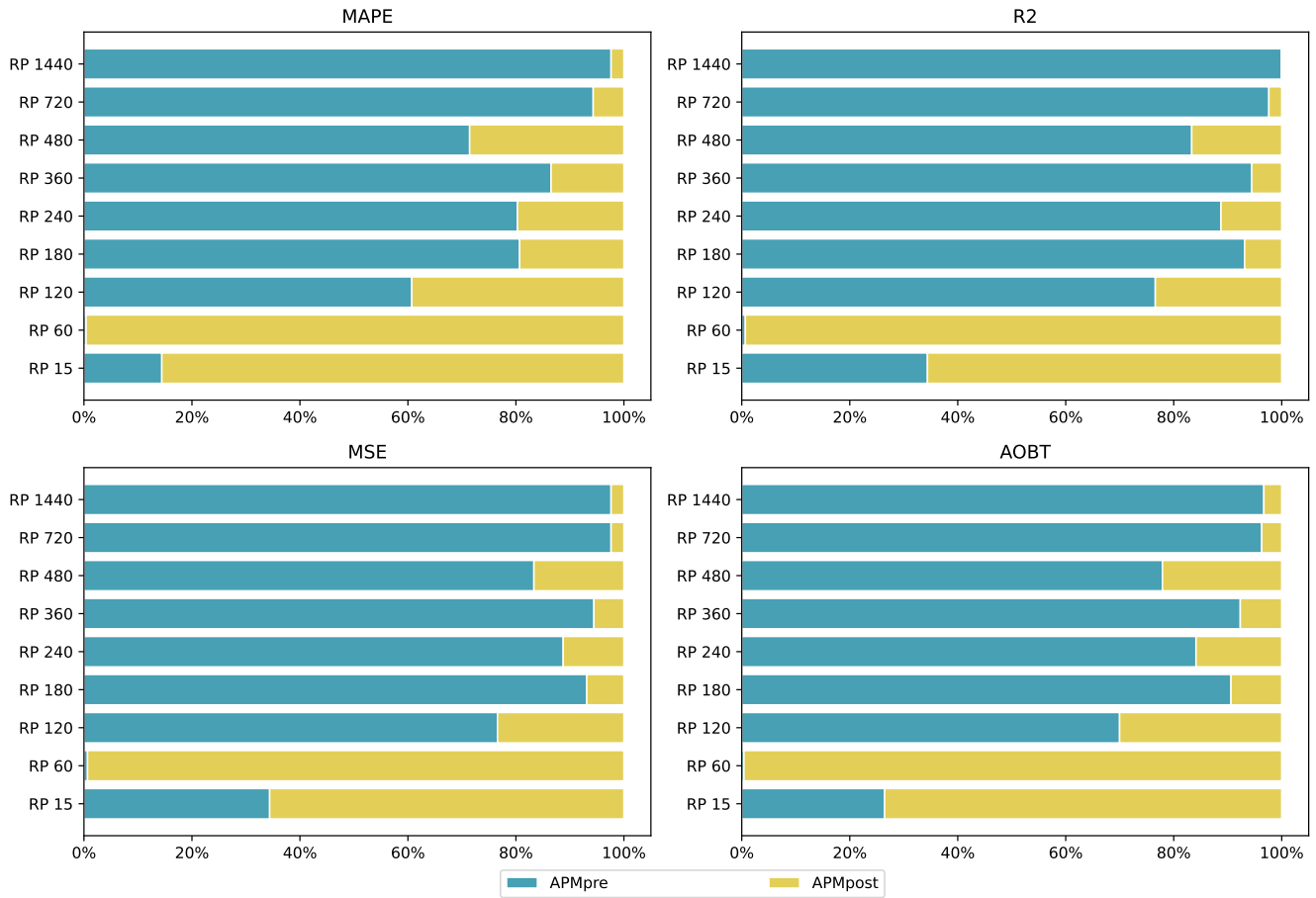


FIGURE 10. Ratio of forecasted timeseries with more accurate predictions of *APMpre* and *APMpost* for various metrics.

and blocked traffic for different amounts of traffic in the networks are presented. Of the total of six, there are two groups of three graphs each. Those on the left-hand side present a set of scenarios for Euro28 topology, *distance* (with timezones applied) traffic type, and 15 000 transceivers in the entire network. On the opposite side, there is a scenario set for US26 topology, *normal* (without timezones applied) traffic type and 15 000 transceivers in the whole network as well. For given scenarios, the overall trend of network capacity for different RPs is presented. As can be seen in the first row, a lower RP gives a lower BBP and, furthermore, a higher capacity of the network. The second row presents the mean frequency slots usage (from the 24-hour traffic) along with 1% BBP represented by dots on the lines as reference points. The third row presents the mean transceiver usage with reference 1% BBP markers. These plots show that, apart from the higher capacity of the network for lower RPs, the usage of resources is also smaller, which gives benefits on all considered sides.

To verify the energy savings, we use the power consumption model proposed in [18]. The example results are presented in Fig. 12. We compared results for 1% BBP for different RPs. It can be seen that the power consumption can

be reduced by 12.5 p.p. for RP = 15 minutes compared to the reference scenario of one-time resource allocation over 24 hours while offering the higher volume of provisioned traffic, i.e. 13.12 EB for RP = 15 minutes vs. 11.47 EB for RP = 24 hours.

Tables 4 and 5 (see appendix) present an evaluation of the BBP and the resources used in the Euro28 and US26 topologies, respectively, for various scenarios adjusted in such a way that the input required group for each group of scenarios (grouped by topology type, traffic type, and number of transceivers) gives the 1% BBP for the lowest RP considered, so the usage of resources can be compared. For all the 24 scenarios presented, parameterized by the type of topology and traffic type, the advantage of using RP is clearly seen, compared to the base approach (no reallocation) represented by RP = 1440 minutes (24 hours).

In terms of BBP, the 15-minute RP performs better than the non-periodic approach with a gain varying from 2.4 p.p. (the lowest gain, US26 topology, traffic type *normal* without timezones, 20 000 transceivers) to even 7.8 p.p. (the highest gain, Euro28 topology, traffic type *normal* without timezones, 15 000 transceivers). Overall, the mean gain in BBP is approx. 5 p.p.

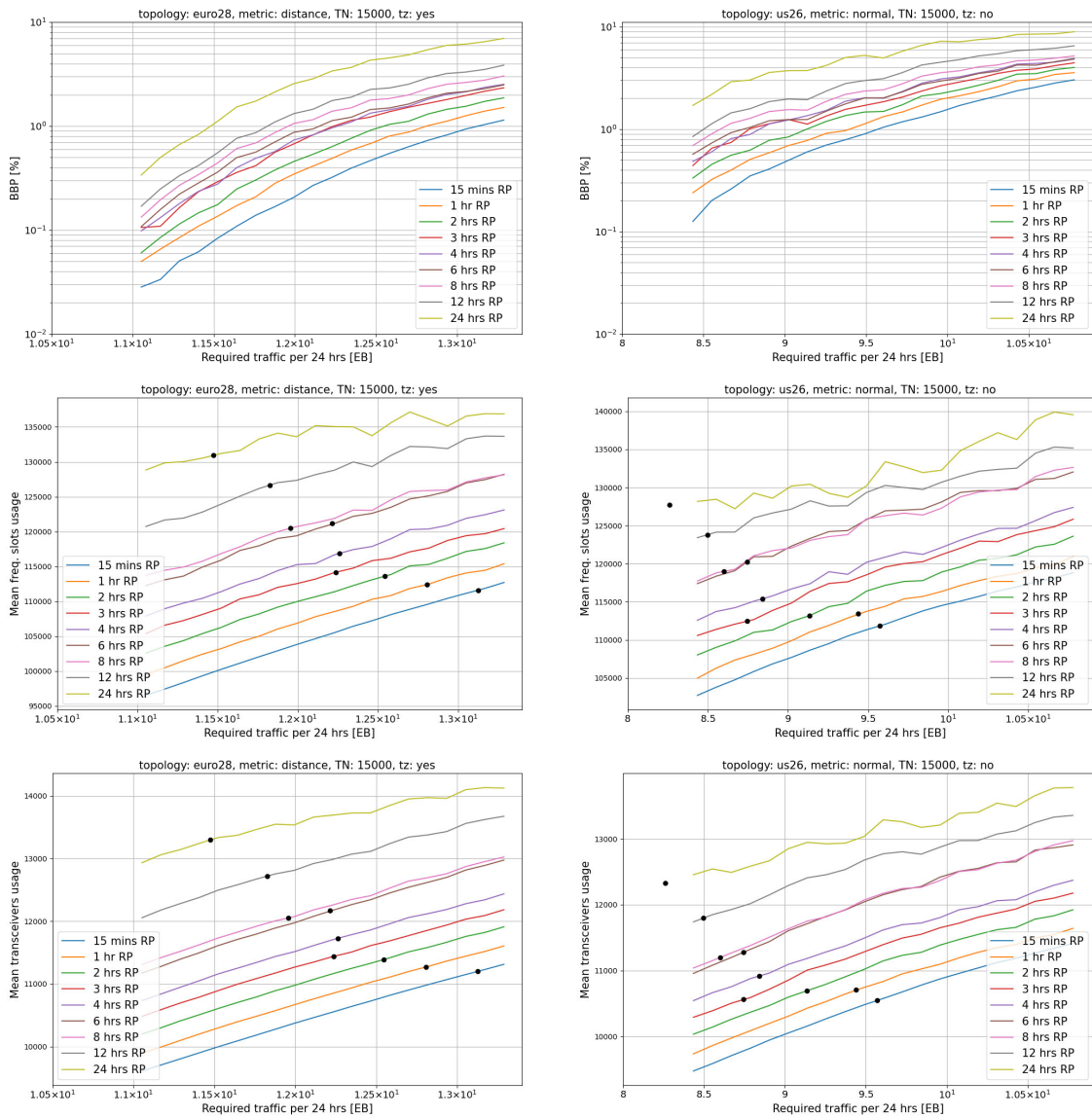


**FIGURE 11.** Comparison of BBP, frequency slots usage and transceivers usage for example scenarios grouped in three figures on left and right hand sides.

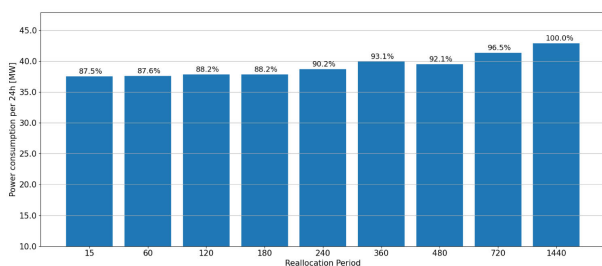


**FIGURE 12.** Energy savings for different reallocation periods for a test configuration consisting of Euro28 topology with 15 000 transceivers for distance traffic with timezones (for 1% BBP).

For mean transceiver usage, the 15-minute RP performs better than the non-periodic approach with lower usage varying from 16.7% (the lowest gain, Euro28 topology,

traffic type *normal* with timezones, 15 000 transceivers) to 23.4% (the highest gain, US26 topology, traffic type *normal* without timezones, 20 000 transceivers). Overall, the mean transceiver usage is lower by the mean value of 19.7%, compared to the base method.

Finally, for mean frequency slots usage, the 15-minute RP performs better than the non-periodic approach with lower usage varying from 11.8% (the lowest gain, Euro28 topology, traffic type *normal* without timezones, 15 000 transceivers) to 19.5% (the highest gain, US26 topology, traffic type *normal* with timezones, 20 000 transceivers). In general, the mean frequency slot usage is lower by the mean value of 16.3%, compared to the base method.

All the results presented above used the baseline approach where 100% traffic prediction is assumed (i.e., the future traffic is known in 100%). The final point of our research



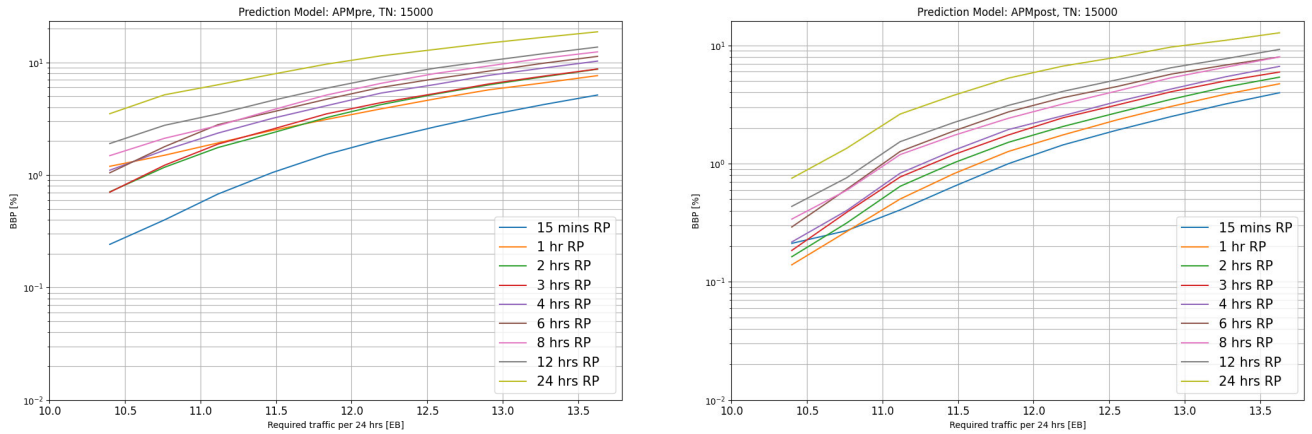


FIGURE 13. BBPs of ARBR + distance\_asc method used with APMpre (left side) and APMpost (right side) prediction models for different RPs.

TABLE 4. Euro28 topology. Evaluation of BBP and used resources: mean used transceivers (MUT), mean used frequency slots (MUFS) for different reallocation periods (RP, in minutes) for method ARBR distance\_asc. Results grouped by traffic type, number of transceivers (TN) and required traffic (Req. Traffic [EB]) that would give 1% BBP for RP = 15 mins.

TN	RP	Traffic type: distance				Traffic type: normal			
		BBP[%]	Req. Traffic	MUT	MUFS	BBP[%]	Req. Traffic	MUT	MUFS
10k	15	1.000	8.6562	7515	75 518	1.000	8.2906	8066	94 810
10k	60	1.324	8.6562	7709	77 365	1.352	8.2906	8256	96 974
10k	120	1.677	8.6562	7909	79 292	1.665	8.2906	8469	99 507
10k	180	2.081	8.6562	8091	80 747	2.174	8.2906	8654	101 422
10k	240	2.300	8.6562	8249	82 424	2.307	8.2906	8820	103 405
10k	360	2.288	8.6562	8612	85 908	2.464	8.2906	9206	108 300
10k	480	2.829	8.6562	8636	85 978	3.000	8.2906	9208	107 916
10k	720	3.624	8.6562	9076	89 752	3.801	8.2906	9656	112 448
10k	1440	6.666	8.6562	9406	91 254	6.552	8.2906	9873	113 822
15k	15	1.000	13.1324	11 206	111 657	1.000	11.5291	11 154	128 518
15k	60	1.346	13.1324	11 495	114 365	1.362	11.5291	11 441	131 076
15k	120	1.674	13.1324	11 802	117 446	1.784	11.5291	11 716	133 626
15k	180	2.115	13.1324	12 069	119 588	2.473	11.5291	11 936	135 775
15k	240	2.299	13.1324	12 319	122 208	2.575	11.5291	12 188	137 929
15k	360	2.252	13.1324	12 863	127 245	2.866	11.5291	12 703	143 742
15k	480	2.732	13.1324	12 925	127 506	3.596	11.5291	12 673	142 708
15k	720	3.454	13.1324	13 602	133 563	4.603	11.5291	13 258	146 717
15k	1440	6.395	13.1324	14 120	136 797	8.803	11.5291	13 400	145 779
20k	15	1.000	16.8559	14 413	139 735	1.000	12.2114	11 950	134 968
20k	60	1.405	16.8559	14 784	144 004	1.364	12.2114	12 274	137 936
20k	120	2.049	16.8559	15 087	143 583	1.758	12.2114	12 604	140 989
20k	180	2.214	16.8559	15 554	150 155	2.288	12.2114	12 841	143 514
20k	240	2.427	16.8559	15 814	151 179	2.465	12.2114	13 148	145 807
20k	360	2.544	16.8559	16 503	158 040	2.501	12.2114	13 725	151 791
20k	480	3.533	16.8559	16 349	153 184	2.993	12.2114	13 784	152 247
20k	720	4.459	16.8559	17 150	159 057	3.766	12.2114	14 562	157 679
20k	1440	7.439	16.8559	17 535	161 823	7.458	12.2114	14 756	158 380
TN	RP	Traffic type: distance with timezones				Traffic type: normal with timezones			
		BBP[%]	Req. Traffic	MUT	MUFS	BBP[%]	Req. Traffic	MUT	MUFS
10k	15	1.000	8.6576	7518	75 540	1.000	8.2987	8074	94 889
10k	60	1.325	8.6576	7711	77 395	1.376	8.2987	8261	97 055
10k	120	1.683	8.6576	7910	79 313	1.676	8.2987	8476	99 621
10k	180	2.088	8.6576	8093	80 778	2.224	8.2987	8658	101 405
10k	240	2.307	8.6576	8252	82 438	2.331	8.2987	8826	103 574
10k	360	2.291	8.6576	8614	86 000	2.477	8.2987	9213	108 362
10k	480	2.833	8.6576	8637	85 961	3.021	8.2987	9213	107 914
10k	720	3.629	8.6576	9077	89 764	3.829	8.2987	9659	112 449
10k	1440	6.672	8.6576	9406	91 267	6.603	8.2987	9875	113 843
15k	15	1.000	13.1255	11 200	111 593	1.000	11.5330	11 160	128 488
15k	60	1.345	13.1255	11 490	114 304	1.385	11.5330	11 439	131 063
15k	120	1.664	13.1255	11 797	117 409	1.792	11.5330	11 716	133 701
15k	180	2.095	13.1255	12 069	119 590	2.531	11.5330	11 936	135 821
15k	240	2.280	13.1255	12 318	122 226	2.595	11.5330	12 190	138 016
15k	360	2.244	13.1255	12 862	127 279	2.861	11.5330	12 715	143 949
15k	480	2.724	13.1255	12 921	127 481	3.617	11.5330	12 671	142 847
15k	720	3.442	13.1255	13 598	133 552	4.632	11.5330	13 258	146 756
15k	1440	6.375	13.1255	14 118	136 777	8.807	11.5330	13 405	145 838
20k	15	1.000	16.7529	14 284	138 779	1.000	12.2069	11 945	134 938
20k	60	1.310	16.7529	14 726	142 519	1.369	12.2069	12 266	137 890
20k	120	1.812	16.7529	15 081	143 076	1.764	12.2069	12 601	140 916
20k	180	2.404	16.7529	15 402	146 786	2.275	12.2069	12 845	143 528
20k	240	2.312	16.7529	15 760	150 881	2.465	12.2069	13 148	145 835
20k	360	2.337	16.7529	16 438	155 344	2.467	12.2069	13 740	151 828
20k	480	3.110	16.7529	16 408	154 143	3.048	12.2069	13 753	152 024
20k	720	3.903	16.7529	17 254	159 583	3.842	12.2069	14 521	157 442
20k	1440	7.104	16.7529	17 501	161 921	7.445	12.2069	14 753	158 391

**TABLE 5. US26 topology. Evaluation of BBP and used resources: mean used transceivers (MUT), mean used frequency slots (MUFS) for different reallocation periods (RP, in minutes) for method *ARBR distance\_asc*. Results grouped by traffic type, number of transceivers (TN) and required traffic (Req. Traffic [EB]) that would give 1% BBP for RP = 15 mins.**

TN	RP	Traffic type: distance				Traffic type: normal			
		BBP[%]	Req. Traffic	MUT	MUFS	BBP[%]	Req. Traffic	MUT	MUFS
10k	15	1.000	8.2641	7589	68 401	1.000	6.6423	7403	80 742
10k	60	1.296	8.2641	7773	69 910	1.315	6.6423	7578	82 332
10k	120	1.551	8.2641	7969	71 662	1.611	6.6423	7771	84 230
10k	180	1.898	8.2641	8140	73 003	1.991	6.6423	7957	85 880
10k	240	2.012	8.2641	8311	74 461	2.225	6.6423	8101	87 108
10k	360	2.060	8.2641	8660	77 560	2.221	6.6423	8459	91 406
10k	480	2.426	8.2641	8694	77 700	2.701	6.6423	8468	90 636
10k	720	3.050	8.2641	9121	80 864	3.442	6.6423	8890	94 067
10k	1440	5.101	8.2641	9435	83 013	5.506	6.6423	9242	95 158
<hr/>									
15k	15	1.000	12.5490	11 350	101 336	1.000	9.5722	10 546	111 826
15k	60	1.282	12.5490	11 634	103 799	1.265	9.5722	10 806	114 198
15k	120	1.536	12.5490	11 936	106 144	1.484	9.5722	11 107	116 925
15k	180	1.893	12.5490	12 203	108 543	1.809	9.5722	11 360	119 246
15k	240	2.051	12.5490	12 440	110 144	2.008	9.5722	11 578	120 650
15k	360	2.130	12.5490	12 972	114 987	2.020	9.5722	12 118	126 584
15k	480	2.527	12.5490	12 998	114 958	2.404	9.5722	12 141	126 164
15k	720	3.148	12.5490	13 637	119 786	3.075	9.5722	12 744	129 982
15k	1440	5.239	12.5490	14 122	122 268	5.044	9.5722	13 211	132 411
<hr/>									
20k	15	1.006	15.9759	14 466	127 772	1.000	10.4565	11 609	122 683
20k	60	1.229	15.9759	14 853	130 876	1.171	10.4565	11 928	125 582
20k	120	1.473	15.9759	15 235	133 985	1.348	10.4565	12 261	128 631
20k	180	1.725	15.9759	15 602	136 946	1.600	10.4565	12 591	131 426
20k	240	1.893	15.9759	15 913	138 961	1.720	10.4565	12 829	133 181
20k	360	1.937	15.9759	16 595	144 958	1.720	10.4565	13 410	138 145
20k	480	2.235	15.9759	16 709	145 217	1.903	10.4565	13 499	138 785
20k	720	2.752	15.9759	17 566	151 128	2.441	10.4565	14 280	145 046
20k	1440	4.492	15.9759	18 250	154 941	3.366	10.4565	15 154	152 315
<hr/>									
TN	RP	Traffic type: distance with timezones				Traffic type: normal with timezones			
		BBP[%]	Req. Traffic	MUT	MUFS	BBP[%]	Req. Traffic	MUT	MUFS
10k	15	1.000	8.2652	7590	68 383	1.000	6.6382	7400	80 733
10k	60	1.290	8.2652	7776	69 965	1.312	6.6382	7573	82 335
10k	120	1.534	8.2652	7975	71 764	1.627	6.6382	7764	84 244
10k	180	1.886	8.2652	8141	73 075	1.994	6.6382	7949	85 926
10k	240	2.003	8.2652	8316	74 537	2.236	6.6382	8094	87 052
10k	360	2.055	8.2652	8669	77 645	2.233	6.6382	8457	91 516
10k	480	2.431	8.2652	8693	77 658	2.687	6.6382	8461	90 488
10k	720	3.057	8.2652	9121	80 860	3.423	6.6382	8889	94 067
10k	1440	5.109	8.2652	9434	83 013	5.487	6.6382	9242	95 183
<hr/>									
15k	15	1.000	12.5478	11 350	101 344	1.000	9.5784	10 555	111 871
15k	60	1.264	12.5478	11 639	103 872	1.258	9.5784	10 815	114 280
15k	120	1.551	12.5478	11 934	106 317	1.496	9.5784	11 114	116 882
15k	180	1.861	12.5478	12 209	108 828	1.786	9.5784	11 369	119 273
15k	240	2.069	12.5478	12 440	110 237	2.015	9.5784	11 595	120 694
15k	360	2.136	12.5478	12 973	115 115	1.983	9.5784	12 137	126 731
15k	480	2.543	12.5478	12 987	114 746	2.414	9.5784	12 155	125 915
15k	720	3.170	12.5478	13 627	119 510	3.091	9.5784	12 745	130 055
15k	1440	5.236	12.5478	14 122	122 275	5.028	9.5784	13 225	132 584
<hr/>									
20k	15	1.000	15.9313	14 431	127 536	1.000	10.4568	11 614	122 644
20k	60	1.207	15.9313	14 817	130 620	1.167	10.4568	11 938	125 665
20k	120	1.443	15.9313	15 207	133 775	1.362	10.4568	12 273	128 595
20k	180	1.671	15.9313	15 586	136 689	1.606	10.4568	12 593	131 464
20k	240	1.849	15.9313	15 889	138 870	1.740	10.4568	12 851	133 349
20k	360	1.890	15.9313	16 573	144 615	1.734	10.4568	13 411	138 117
20k	480	2.164	15.9313	16 676	144 875	1.935	10.4568	13 490	138 757
20k	720	2.669	15.9313	17 542	150 889	2.456	10.4568	14 268	144 930
20k	1440	4.359	15.9313	18 235	154 712	3.369	10.4568	15 153	152 317

is to combine the tuned method *ARBR distance\_asc* with the prediction models proposed in Section V to verify how the proposed, fine-tuned allocation algorithm performs in the realistic scenario with incomplete knowledge about the incoming time-varying traffic. To recall, the predicted traffic, represented as the required bandwidths for each node pair in a given RP, is used in the ARBR algorithm as a parameter for allocating lightpaths according to those predicted requests. For this case, we consider the Euro28 topology with a network of 15 000 transceivers along with *APMpre* and *APMpost* models tested for different traffic loads with an additional 10% overhead of predicted values for each pair of nodes, as described at the end of Section VI-C). The results presented in Fig. 13 show that our proposed method works with traffic prediction methods that preserve the gain in

network capacity depending on the applied RP and the trends that occurred in the synthetic tests presented in previous Sections.

### VII. CONCLUSION

In this paper, we proposed an optimization method to improve the performance of the translucent elastic optical network with traffic that varies in time. Based on extensive research, including the analysis of different aspects of the optical network resource optimization methods and machine learning methods, we designed the dynamic allocation algorithm that manages the resources of the network using the traffic prediction models. Starting from several semi-synthetic data sets that mimic the real varying nature of the networking demands, we introduced the concept of periodic allocation

and enhanced versions of the dynamic routing ARBR algorithm, which were tested against different scenarios, including different topologies, traffic types, and number of resources used in the network. Then, we focus on traffic prediction methods that would provide reliable information about incoming traffic in the next time range. Finally, we combined all the elements mentioned to test our method in simulations to prove that it works properly.

The proposed method performs better in terms of bandwidth blocking probability and resource usage compared to the standard one-time allocation approach (with RP = 24 hours). It is important to mention that this approach does not require any additional resources in the given network, so the application of such a method can be quickly done in cognitive networks, e.g., software-defined networks. We evaluated that the gain of usage our approach, in terms of BBP, can be around 7.8 p.p., compared to a one-time allocation approach (without reallocation), with the use of 23.4% less transceivers, 19.5% less frequency slots, and less consumed power by transceivers.

The results presented above clearly confirm that the idea of periodic reallocation of light paths due to changing traffic provides benefits. However, in this work, as an initial study, we made some simplifications, i.e., we assume that the time required for network reconfiguration is not taken into account. Therefore, in future work, we plan to propose and evaluate an optimization framework for hit-less reallocation scheme that will address more detailed constraints of the network reconfiguration process. In addition, we will analyze various criteria that can be used for triggering the reallocation in the network, since this approach could reduce the number of reallocations without reduction of the key performance metrics. Moreover, we plan to focus on a more accurate traffic prediction.

## APPENDIX TABLES

Tables 4 and 5.

## REFERENCES

- [1] *The Mobile Internet Phenomena Report*, Sandvine, Waterloo, ON, Canada, May 2021.
- [2] *The Nokia Deepfield Network Intelligence Report 2020*, NOKIA, Espoo, Finland, 2020.
- [3] (Apr. 2024). *Seattle Internet Exchange*. [Online]. Available: <https://www.seattleix.net/statistics/>
- [4] T. Panayiotou, M. Michalopoulou, and G. Ellinas, "Survey on machine learning for traffic-driven service provisioning in optical networks," *IEEE Commun. Surveys Tuts.*, vol. 25, no. 2, pp. 1412–1443, 2nd Quart., 2023.
- [5] F. Musumeci, C. Rottondi, A. Nag, I. Macaluso, D. Zibar, M. Ruffini, and M. Tornatore, "An overview on application of machine learning techniques in optical networks," *IEEE Commun. Surveys Tuts.*, vol. 21, no. 2, pp. 1383–1408, 2nd Quart., 2019.
- [6] M. Ibrahim, C. Rottondi, and M. Tornatore, "Machine learning methods for quality-of-transmission estimation," in *Machine Learning for Future Fiber-Optic Communication Systems*. Amsterdam, The Netherlands: Elsevier, 2022, pp. 189–224.
- [7] I. Sartzetakis, K. K. Christodoulou, and E. M. Varvarigos, "Accurate quality of transmission estimation with machine learning," *J. Opt. Commun. Netw.*, vol. 11, no. 3, pp. 140–150, Mar. 2019.
- [8] E. Etezadi, C. Natalino, R. Diaz, A. Lindgren, S. Melin, L. Wosinska, P. Monti, and M. Furdek, "DeepDefrag: A deep reinforcement learning framework for spectrum defragmentation," in *Proc. IEEE Global Commun. Conf.*, Dec. 2022, pp. 3694–3699.
- [9] P. Lechowicz, "Regression-based fragmentation metric and fragmentation-aware algorithm in spectrally-spatially flexible optical networks," *Comput. Commun.*, vol. 175, pp. 156–176, Jul. 2021.
- [10] S. Wojciechowski, R. Goscienn, P. Ksieniewicz, and K. Walkowiak, "Hybrid regression model for link dimensioning in spectrally-spatially flexible optical networks," *IEEE Access*, vol. 10, pp. 53810–53821, 2022.
- [11] P. Ksieniewicz, R. Gościński, M. Klinkowski, and K. Walkowiak, "Pattern recognition model to aid the optimization of dynamic spectrally-spatially flexible optical networks," in *Proc. Int. Conf. Comput. Sci.* Cham, Switzerland: Springer, 2020, pp. 211–224.
- [12] A. Valkanis, G. Papadimitriou, P. Nicopolitidis, G. A. Beletsioti, and E. Varvarigos, "A traffic prediction assisted routing algorithm for elastic optical networks," in *Proc. Int. Conf. Commun., Comput., Cybersecurity, Informat. (CCCI)*, Oct. 2021, pp. 1–6.
- [13] F. Morales, P. Festa, M. Ruiz, and L. Velasco, "Adapting the virtual network topology to near future traffic," in *Proc. 19th Int. Conf. Transparent Opt. Netw. (ICTON)*, Jul. 2017, pp. 1–4.
- [14] M. Aibin, N. Chung, T. Gordon, L. Lyford, and C. Vinchoff, "On short- and long-term traffic prediction in optical networks using machine learning," in *Proc. Int. Conf. Opt. Netw. Design Modelling (ONDM)*, Jun. 2021, pp. 1–6.
- [15] P. Lechowicz, R. Goscienn, R. Rumipamba-Zambrano, J. Perello, S. Spadaro, and K. Walkowiak, "Greenfield gradual migration planning toward spectrally-spatially flexible optical networks," *IEEE Commun. Mag.*, vol. 57, no. 10, pp. 14–19, Oct. 2019.
- [16] M. Ruiz, L. Velasco, A. Lord, D. Fonseca, M. Pioro, R. Wessaly, and J. P. Fernandez-palacios, "Planning fixed to flexgrid gradual migration: Drivers and open issues," *IEEE Commun. Mag.*, vol. 52, no. 1, pp. 70–76, Jan. 2014.
- [17] M. Klinkowski, P. Lechowicz, and K. Walkowiak, "Survey of resource allocation schemes and algorithms in spectrally-spatially flexible optical networking," *Opt. Switching Netw.*, vol. 27, pp. 58–78, Jan. 2018.
- [18] Y. Xiong, J. Shi, Y. Yang, Y. Lv, and G. N. Rouskas, "Lightpath management in SDN-based elastic optical networks with power consumption considerations," *J. Lightw. Technol.*, vol. 36, no. 9, pp. 1650–1660, May 15, 2018.
- [19] R. Ramaswami, K. N. Sivarajan, and G. H. Sasaki, *Optical Networks: A Practical Perspective*, 3rd ed., San Mateo, CA, USA: Morgan Kaufmann, 2009.
- [20] K. Christodoulou, K. Manousakis, and E. Varvarigos, "Offline routing and wavelength assignment in transparent WDM networks," *IEEE/ACM Trans. Netw.*, vol. 18, no. 5, pp. 1557–1570, Oct. 2010.
- [21] K. Manousakis, P. Kokkinos, K. Christodoulou, and E. Varvarigos, "Joint online routing, wavelength assignment and regenerator allocation in translucent optical networks," *J. Lightw. Technol.*, vol. 28, no. 8, pp. 1152–1163, Apr. 1, 2010.
- [22] J. Perelló, J. M. Gené, A. Pagès, J. A. Lazaro, and S. Spadaro, "Flex-grid/SDM backbone network design with inter-core XT-limited transmission reach," *J. Opt. Commun. Netw.*, vol. 8, no. 8, pp. 540–552, Aug. 2016.
- [23] H. Tode and Y. Hirota, "Routing, spectrum, and core and/or mode assignment on space-division multiplexing optical networks [invited]," *J. Opt. Commun. Netw.*, vol. 9, no. 1, pp. A99–A113, Jan. 2017.
- [24] F. Pederzoli, D. Siracusa, J. M. Rivas-Moscoso, B. Shariati, E. Salvadori, and I. Tomkos, "Spatial group sharing for SDM optical networks with joint switching," in *Proc. Int. Conf. Opt. Netw. Design Model. (ONDM)*, May 2016, pp. 1–6.
- [25] B. Shariati, D. Klondis, D. Siracusa, F. Pederzoli, J. M. Rivas-Moscoso, L. Velasco, and I. Tomkos, "Impact of traffic profile on the performance of spatial superchannel switching in SDM networks," in *Proc. 42nd Eur. Conf. Opt. Commun.*, Sep. 2016, pp. 1–3.
- [26] F. Pederzoli, D. Siracusa, B. Shariati, J. M. Rivas-Moscoso, E. Salvadori, and I. Tomkos, "Improving performance of spatially joint-switched space division multiplexing optical networks via spatial group sharing," *J. Opt. Commun. Netw.*, vol. 9, no. 3, pp. B1–B11, Mar. 2017.
- [27] F. Pederzoli, M. Gerola, A. Zanardi, X. Forns, J. F. Ferran, and D. Siracusa, "YAMATO: The first SDN control plane for independent, joint, and fractional-joint switched SDM optical networks," *J. Lightw. Technol.*, vol. 35, no. 8, pp. 1335–1341, Apr. 1, 2017.

- [28] G. M. Saridis, D. Alexandropoulos, G. Zervas, and D. Simeonidou, "Survey and evaluation of space division multiplexing: From technologies to optical networks," *IEEE Commun. Surveys Tuts.*, vol. 17, no. 4, pp. 2136–2156, 4th Quart., 2015.
- [29] A. Muhammad, G. Zervas, and R. Forchheimer, "Resource allocation for space-division multiplexing: Optical white box versus optical black box networking," *J. Lightw. Technol.*, vol. 33, no. 23, pp. 4928–4941, Dec. 15, 2015.
- [30] H. Zang, J. P. Jue, and B. Mukherjee, "A review of routing and wavelength assignment approaches for wavelength-routed optical WDM networks," *Opt. Netw.*, vol. 1, no. 1, pp. 47–60, 2000.
- [31] G. Zhang, M. De Leenheer, A. Morea, and B. Mukherjee, "A survey on OFDM-based elastic core optical networking," *IEEE Commun. Surveys Tuts.*, vol. 15, no. 1, pp. 65–87, 1st Quart., 2013.
- [32] B. C. Chatterjee, N. Sarma, and E. Oki, "Routing and spectrum allocation in elastic optical networks: A tutorial," *IEEE Commun. Surveys Tuts.*, vol. 17, no. 3, pp. 1776–1800, 3rd Quart., 2015.
- [33] A. Zapata and S. Ahumada, "Static vs. dynamic wavelength-routed optical networks under time-varying traffic," in *Proc. Conf. Opt. Fiber Communication/National Fiber Optic Engineers Conf.*, Feb. 2008, pp. 1–3.
- [34] J. Weigu, H. Shanguo, Z. Jie, Z. Yunfan, and Z. Chenming, "Dynamic time-varying spectrum allocation algorithm in flexible grid optical networks," in *Proc. 15th Int. Conf. Opt. Commun. Netw. (ICOON)*, Sep. 2016, pp. 1–3.
- [35] S. Zhang, M. Tornatore, G. Shen, J. Zhang, and B. Mukherjee, "Evolving traffic grooming in multi-layer flexible-grid optical networks with software-defined elasticity," *J. Lightw. Technol.*, vol. 32, no. 16, pp. 2905–2914, Aug. 15, 2014.
- [36] C. Rožic, D. Klionidis, and I. Tomkos, "A survey of multi-layer network optimization," in *Proc. Int. Conf. Opt. Netw. Design Model. (ONDM)*, May 2016, pp. 1–6.
- [37] A. Knapieńska, P. Lechowicz, S. Spadaro, and K. Walkowiak, "Performance analysis of multilayer optical networks with time-varying traffic," in *Proc. 23rd Int. Conf. Transparent Opt. Netw. (ICTON)*, Jul. 2023, pp. 1–4.
- [38] I. Lohrasbinasab, A. Shahraiki, A. Taherkordi, and A. D. Jurcut, "From statistical-to machine learning-based network traffic prediction," *Trans. Emerg. Telecommun. Technol.*, vol. 33, no. 4, p. e4394, 2022.
- [39] G. O. Ferreira, C. Ravazzi, F. Dabbene, G. C. Calafiore, and M. Fiore, "Forecasting network traffic: A survey and tutorial with open-source comparative evaluation," *IEEE Access*, vol. 11, pp. 6018–6044, 2023.
- [40] A. Knapieńska, P. Lechowicz, W. Węgiel, and K. Walkowiak, "Long-term prediction of multiple types of time-varying network traffic using chunk-based ensemble learning," *Appl. Soft Comput.*, vol. 130, Nov. 2022, Art. no. 109694.
- [41] D. Szostak, A. Włodarczyk, and K. Walkowiak, "Machine learning classification and regression approaches for optical network traffic prediction," *Electronics*, vol. 10, no. 13, p. 1578, Jun. 2021.
- [42] S. Troia, R. Alvizu, Y. Zhou, G. Maier, and A. Pattavina, "Deep learning-based traffic prediction for network optimization," in *Proc. 20th Int. Conf. Transparent Opt. Netw. (ICTON)*, Jul. 2018, pp. 1–4.
- [43] H. Khodakarami, B. S. G. Pillai, and W. Shieh, "Quality of service provisioning and energy minimized scheduling in software defined flexible optical networks," *J. Opt. Commun. Netw.*, vol. 8, no. 2, pp. 118–128, Feb. 2016.
- [44] S. K. Singh and A. Jukan, "Machine-learning-based prediction for resource (re)allocation in optical data center networks," *J. Opt. Commun. Netw.*, vol. 10, no. 10, pp. D12–D28, Oct. 2018.
- [45] A. Knapieńska, P. Lechowicz, S. Spadaro, and K. Walkowiak, "On advantages of traffic prediction and grooming for provisioning of time-varying traffic in multilayer networks," in *Proc. Int. Conf. Opt. Netw. Design Modelling (ONDM)*, May 2023, pp. 1–6.
- [46] D. Andreoletti, S. Troia, F. Musumeci, S. Giordano, G. Maier, and M. Tornatore, "Network traffic prediction based on diffusion convolutional recurrent neural networks," in *Proc. IEEE Conf. Comput. Commun. Workshops (INFOCOM WKSHPS)*, Apr. 2019, pp. 246–251.
- [47] K. Lei, M. Qin, B. Bai, G. Zhang, and M. Yang, "GCN-GAN: A non-linear temporal link prediction model for weighted dynamic networks," in *Proc. IEEE Conf. Comput. Commun.*, Apr. 2019, pp. 388–396.
- [48] A. Knapieńska, P. Lechowicz, A. Włodarczyk, and K. Walkowiak, "Data aggregation and clustering for traffic prediction in backbone optical networks," in *Proc. 27th Int. Conf. Opt. Netw. Design Modelling (ONDM)*, 2023, pp. 1–3.
- [49] K. Walkowiak, M. Klinkowski, and P. Lechowicz, "Dynamic routing in spectrally spatially flexible optical networks with back-to-back regeneration," *J. Opt. Commun. Netw.*, vol. 10, no. 5, pp. 523–534, May 2018.
- [50] D. Szostak, K. Walkowiak, and A. Włodarczyk, "Short-term traffic forecasting in optical network using linear discriminant analysis machine learning classifier," in *Proc. 22nd Int. Conf. Transparent Opt. Netw. (ICTON)*, Jul. 2020, pp. 1–4.
- [51] P. S. Khodashenas, J. M. Rivas-Moscoco, D. Siracusa, F. Pederzoli, B. Shariati, D. Klionidis, E. Salvadori, and I. Tomkos, "Comparison of spectral and spatial super-channel allocation schemes for SDM networks," *J. Lightw. Technol.*, vol. 34, no. 11, pp. 2710–2716, Jun. 1, 2016.
- [52] T. Zami, A. Morea, and J. Pesic, "Benefit of progressive deployment of regenerators along with traffic growth in WDM elastic networks," in *Proc. Opt. Fiber Commun. Conf. Expo. (OFC)*, Mar. 2018, pp. 1–3.
- [53] A. Włodarczyk, P. Lechowicz, D. Szostak, and K. Walkowiak, "An algorithm for provisioning of time-varying traffic in translucent SDM elastic optical networks," in *Proc. 22nd Int. Conf. Transparent Opt. Netw. (ICTON)*, Jul. 2020, pp. 1–4.
- [54] *Cisco Annual Internet Report 2018–2023*, Cisco Company, San Jose, CA, USA, Mar. 2020.
- [55] A. Deore, O. Turkcü, S. Ahuja, S. J. Hand, and S. Melle, "Total cost of ownership of WDM and switching architectures for next-generation 100 Gb/s networks," *IEEE Commun. Mag.*, vol. 50, no. 11, pp. 179–187, Nov. 2012.
- [56] P. Pavon-Marino, B. Garcia-Manrubia, and R. Aparicio-Pardo, "Multi-hour network planning based on domination between sets of traffic matrices," *Comput. Netw.*, vol. 55, no. 3, pp. 665–675, Feb. 2011.
- [57] M. Klinkowski, M. Ruiz, L. Velasco, D. Careglio, V. Lopez, and J. Comellas, "Elastic spectrum allocation for time-varying traffic in FlexGrid optical networks," *IEEE J. Sel. Areas Commun.*, vol. 31, no. 1, pp. 26–38, Jan. 2013.
- [58] K. Christodoulouopoulos, I. Tomkos, and E. A. Varvarigos, "Routing and spectrum allocation in OFDM-based optical networks with elastic bandwidth allocation," in *Proc. IEEE Global Telecommun. Conf. (GLOBECOM)*, Dec. 2010, pp. 1–6.
- [59] M. Klinkowski and K. Walkowiak, "Routing and spectrum assignment in spectrum sliced elastic optical path network," *IEEE Commun. Lett.*, vol. 15, no. 8, pp. 884–886, Aug. 2011.
- [60] K. Walkowiak, *Modeling and Optimization of Cloud-Ready and Content-Oriented Networks*, vol. 56. Cham, Switzerland: Springer, 2016.
- [61] K. Walkowiak, P. Lechowicz, and M. Klinkowski, "Survivable routing in spectrally-spatially flexible optical networks with back-to-back regeneration," in *Proc. 10th Int. Workshop Resilient Netw. Design Modelling (RNDM)*, Aug. 2018, pp. 1–8.
- [62] K. Walkowiak, P. Lechowicz, and M. Klinkowski, "Transceiver sharing in survivable spectrally-spatially flexible optical networks," in *Proc. IEEE Global Commun. Conf. (GLOBECOM)*, Dec. 2018, pp. 1–6.
- [63] M. Aibin and K. Walkowiak, "Adaptive modulation and regenerator-aware dynamic routing algorithm in elastic optical networks," in *Proc. IEEE Int. Conf. Commun. (ICC)*, Jun. 2015, pp. 5138–5143.
- [64] A. S. Thyagaturu, A. Mercian, M. P. McGarry, M. Reisslein, and W. Kellerer, "Software defined optical networks (SDONs): A comprehensive survey," *IEEE Commun. Surveys Tuts.*, vol. 18, no. 4, pp. 2738–2786, 4th Quart., 2016.
- [65] M. Nance Hall, K.-T. Foerster, S. Schmid, and R. Durairajan, "A survey of reconfigurable optical networks," *Opt. Switching Netw.*, vol. 41, Sep. 2021, Art. no. 100621.
- [66] Z. Wu, S. Pan, F. Chen, G. Long, C. Zhang, and P. S. Yu, "A comprehensive survey on graph neural networks," *IEEE Trans. Neural Netw. Learn. Syst.*, vol. 32, no. 1, pp. 4–24, Jan. 2021.
- [67] A. Knapieńska, P. Lechowicz, and K. Walkowiak, "Machine-learning based prediction of multiple types of network traffic," in *Proc. 21st Int. Conf. Comput. Sci. (ICCS)*. Cham, Switzerland: Springer, 2021, pp. 122–136.
- [68] H. Borchani, G. Varando, C. Bielza, and P. Larrañaga, "A survey on multi-output regression," *Wiley Interdiscipl. Rev., Data Mining Knowl. Discovery*, vol. 5, no. 5, pp. 216–233, 2015.
- [69] A. Knapieńska, O. Ayoub, C. Rottondi, P. Lechowicz, and K. Walkowiak, "Explainable artificial intelligence-guided optimization of ML-based traffic prediction," in *Proc. 28th Int. Conf. Opt. Netw. Design Modelling (ONDM)*, 2024, pp. 1–6.
- [70] A. Knapieńska, P. Lechowicz, S. Spadaro, and K. Walkowiak, "Agnostic prediction of multiple types of time-varying traffic in optical networks," in *Proc. IEEE Global Commun. Conf.*, Dec. 2023, pp. 1131–1136.

- [71] X. Hu, L. Chu, J. Pei, W. Liu, and J. Bian, "Model complexity of deep learning: A survey," *Knowl. Inf. Syst.*, vol. 63, no. 10, pp. 2585–2619, Oct. 2021.
- [72] Y. Fan, X. Pang, A. Udalcovs, C. Natalino, L. Zhang, S. Spolitis, V. Bobrovs, R. Schatz, X. Yu, M. Furdek, S. Popov, and O. Ozolins, "Linear regression vs. deep learning for signal quality monitoring in coherent optical systems," *IEEE Photon. J.*, vol. 14, no. 4, pp. 1–8, Aug. 2022.
- [73] R. Gościński, "Traffic-aware service relocation in software-defined and intent-based elastic optical networks," *Comput. Netw.*, vol. 225, Apr. 2023, Art. no. 109660.
- [74] H. Yang, X. Li, W. Qiang, Y. Zhao, W. Zhang, and C. Tang, "A network traffic forecasting method based on SA optimized ARIMA-BP neural network," *Comput. Netw.*, vol. 193, Jul. 2021, Art. no. 108102.
- [75] A. Knapinska, P. Lechowicz, and K. Walkowiak, "Prediction of multiple types of traffic with a novel evaluation metric related to bandwidth blocking," in *Proc. IEEE Global Commun. Conf.*, Dec. 2022, pp. 2927–2932.
- [76] M. Klinkowski, J. Perelló, and D. Careglio, "Application of linear regression in latency estimation in packet-switched 5G xHaul networks," in *Proc. 23rd Int. Conf. Transparent Opt. Netw. (ICTON)*, Jul. 2023, pp. 1–4.



**ADAM WŁODARCZYK** received the M.Sc. degree from Wrocław University of Science and Technology (WrocławTech), in 2017, where he is currently pursuing the Ph.D. degree with the Doctoral School. He is currently a Research and Teaching Assistant with the Department of Systems and Computer Networks, WrocławTech. His research interests include optical network optimization, meta-heuristic algorithms, and parallel computing.



**ALEKSANDRA KNAPIŃSKA** (Member, IEEE) received the M.Sc. degree from Wrocław University of Science and Technology (WrocławTech), in 2020, where she is currently pursuing the Ph.D. degree with the Doctoral School. She is currently a Research and Teaching Assistant with the Department of Systems and Computer Networks, WrocławTech. Her research interest includes the application of machine learning techniques in optical network optimization.



**PIOTR LECHOWICZ** (Member, IEEE) received the M.Sc. and Ph.D. degrees from Wrocław University of Science Technology (WrocławTech), in 2016 and 2019, respectively. Currently, he is a Postdoctoral Fellow with the Optical Networks (ON) Unit, Department of Electrical Engineering, Chalmers University of Technology. He is the co-author of 35 publications, including ten articles from the JCR list. His research interests include the modeling and optimization of optical networks, spectrally-spatially flexible optical networks, and network fragmentation.



**KRZYSZTOF WALKOWIAK** (Senior Member, IEEE) received the Ph.D. and D.Sc. (Habilitation) degrees from Wrocław University of Science and Technology (WrocławTech), in 2000 and 2008, respectively. He is currently a Professor with the Department of Systems and Computer Networks, WrocławTech. He has co-authored above 320 articles, 75 of them published in JCR journals. His research interests include optimization of communication networks, machine learning, and intent-based networks. He received the 2014 Fabio Neri Best Paper Award.

...